DYNAMICS OF CLIMATE, PHENOLOGY, AND PRODUCTIVITY ACROSS A HYDROLOGIC GRADIENT IN A MONTANE MEADOW

A Thesis submitted to the faculty of
San Francisco State University
In partial fulfillment of
the requirements for
the Degree

Master of Arts

In

Geography

by

Chloe S. Martin

San Francisco, California

August 2022

Certification of Approval

I certify that I have read Dynamics of Climate, Phenology, and Productivity Across a Hydrologic Gradient in a Montane Meadow by Chloe S. Martin, and that in my opinion this work meets the criteria for approving a thesis submitted in partial fulfillment of the requirement for the degree Master of Arts in Geography at San Francisco State University.

_____

Sara Baguskas, Ph.D.
Assistant Professor,
Thesis Committee Chair

_____

Kevin Simonin, Ph.D.
Associate Professor

_____

Jerry Davis, Ph.D.
Professor

Dynamics of Climate, Phenology, and Productivity Across a Hydrologic Gradient in a Montane Meadow

Chloe S. Martin
San Francisco, California
2022

In the Sierra Nevada, restoration of degraded montane meadows has the potential to increase water availability, improving meadow productivity and resilience against climate change. The objective of this study was to evaluate the impact of water availability on growing season timing and duration in a montane meadow ecosystem undergoing restoration. Plant productivity, water availability, and environmental variables were examined at several scales along a hydrologic gradient in Red Clover Valley, California. Field data were collected from May-August 2021, and NDGI was used to compare years 2018-2021. Analysis of the 2021 growing season indicates that environmental controls vary by plant group, with community changes occurring throughout the season. In 2021, a year of severe drought, VPD limited productivity, even with higher water availability and the growing season was shorter, earlier, with lower peak productivity. Results highlight controls on meadow vegetation and establishes a baseline of productivity metrics useful for comparison and ongoing monitoring efforts.

Preface and/or Acknowledgements

Thank you to all who made this project possible. A big thanks to Sara for all the guidance and expertise that shaped this project, and the enthusiasm that kept me going. Thank you to my committee for your valuable feedback from the beginning to the end of this project. Thanks to Andrew Oliphant for the help collecting belowground biomass samples, for allowing my use of the chamber and eddy flux tower data, and to those who assisted in the collection thereof. Thanks to Terri Rust for invaluable context on the site and its flora. This project was funded by the California Climate Investments and California Department of Fish and Wildlife Wetlands Restoration for Greenhouse Gas Reduction fund and is a part of The Sierra Fund's Ecosystem and Community Resiliency in the Sierra Nevada: Restoration of the Clover Valley Ranch Project (grant agreement Q1996007). I would like to acknowledge the landowners Red Clover LLC and additional project partners that helped make this project possible, funding for the meadow restoration work came from the Natural Resource Conservation Service, the Wildlife Conservation Board, and the United States Fish and Wildlife Service. This project takes place on the traditional homelands of the Maidu. Lastly, a special thank you to my partner Julian who assisted me in the field, my family, Myriam, Joel, and Lux – thank you all for your unwavering support and belief in my capability.

Table of Contents

List of Tables

List of Figures

List of Appendices

1. Introduction

1.1 Climate change and high-altitude semi-arid grasslands and meadows

With warming of 0.78 °C occurring from 1850 to 2012, and additional near-term warming of 0.3 °C to 0.7 °C by 2035 (IPCC, 2013), climate change ushers in rising temperatures, sea levels, and uncertainty. Through changes in temperature and global weather patterns, climate change heralds changes to vegetation distribution, productivity, and species survival. On a global scale, we see general patterns in species range shifts with latitude and altitude (IPCC, 2013; Kottek et al., 2006), as plant species distributions are altered to stay within their respective temperature requirements for growth and reproduction. Climate change projections and their implications differ around the globe, with precipitation increasing in some regions, but decreasing in others (IPCC, 2013), and with rates of warming occurring unevenly (Bussotti et al., 2014). In terms of vegetation productivity, there is a similar heterogeneity in predicted impacts. In the far north and south, which are largely limited by low temperatures, productivity and biomass are expected to increase with rising temperatures (Bussotti et al., 2014). In water-limited arid and semiarid climates, however, warmer and drier conditions could lead to decreases in productivity. As such, changes in water availability are particularly important to understand how increasing temperatures will impact vegetation, both in terms of productivity and species survival.

In both grasslands and meadows ecosystems, grasses are a significant component of the vegetation community. However, grasses have variable rooting depths, with more shallow-rooted species being more sensitive to periods of drought, raising questions about community composition stability during drought (Li et al., 2020), particularly in areas where droughts are

becoming more frequent. Thus, changes in precipitation timing and amount are expected to have significant implications for meadow structure and overall productivity but the outcomes are uncertain. For example, previous work in montane meadow systems has shown the timing of precipitation can have a greater effect than changes in annual precipitation on net ecosystem productivity (NEP) (Sloat et al., 2015). In addition, water availability during a particular growing season is not limited to annual precipitation as rainfall in the preceding fall can have significant impacts on leaf and flower formation in the following spring (Jonas et al., 2008) which has subsequent effects on meadow carbon fluxes (Sloat et al., 2015).

For meadows at high altitudes, winter snowpack is extremely important, with snow, snow-up and snowmelt, quantity, and depth all being important contributions to water availability and thus, vegetation productivity. In one experiment during a five-year drought, aboveground biomass of grasses (*Poaceae* spp.) decreased significantly, with deeper-rooting forbs faring much better. In comparison, results showed that where snow was deeper, there was an increase in root biomass and net ecosystem exchange (NEE), with community composition remaining markedly more stable (Li et al., 2020). Though later snowmelt did not appear to impede vegetation growth in this context, a study in the Swiss Alps found that later snowmelt led to more diminutive vegetation, and earlier snowmelt with the domination of taller and faster-growing plants (Jonas et al., 2008).

Winter snowpack is especially important in areas that receive little spring and summer rainfall (i.e., seasonally dry climates), as snowmelt can persist in deep soil horizons and serve as a water source for vegetation through extended dry periods. In wet-summer areas such as Inner Mongolia, deepening snow translated to increased soil moisture which helped sustain vegetation

until the wet season (Li et al., 2020). In dry-summer regions such as California, earlier snowmelt can mean a decrease in net ecosystem productivity (NEP), as there is more time without water, with higher temperatures enhancing soil drying (Sloat, et al., 2015; Arnold, 2014, p.8).

Timing of precipitation is another key element that affects plant productivity. A watering experiment with montane meadow vegetation found precipitation timing was more significant than total amount in influencing NEP for meadow vegetation (Sloat et al., 2015). Water availability during one growing season is not the only factor impacting plant growth, with previous seasons' precipitation also having an impact. In a Swiss Alp study primarily examining meadows showed that rainfall in the preceding fall impacted leaf and flower formation in the spring, as these had pre-formed before snow-up (Jonas et al., 2008). In addition, this has been seen to influence meadow carbon fluxes (Sloat et al., 2015).

Drier conditions and insufficient water supply, either from reductions in rain, snow, or a combination thereof, have further implications for soil health and composition in addition to soil moisture. Soil drying has been linked with a decrease in peak season carbon uptake (Sloat, et al., 2015). The earlier onset of spring spurred by higher surface temperatures also leads to shifts in timing, namely earlier phenology and snowmelt, the latter translating to decreased soil moisture (Sloat et al., 2015; Wang et al., 2020). Estimates of spring advancement observed in recent decades vary, ranging between 2.8 to 5.1 days per decade (Cleland et al., 2007). The impacts of spring advancement are unclear, and several studies have examined whether this will translate into a longer growing season overall. However, it has been observed in some areas to come in tandem with an earlier senescence, offsetting any potential gains in biomass production. A study in the alpine grasslands of China observed that earlier start of the growing season over several

decades caused a compression of the growth period, with changes in grass, sedge, and forb response leading to changes in abundance (Wang et al., 2020). In other cases, increased productivity in spring is outweighed by decreased productivity in summer, the overall decrease of NEP linked to warming and drier soils (Sloat et al., 2015).

1.2 California's montane meadows

Montane meadows in California provide significant ecosystem services in the Sierra Nevada and the state at large, as important areas for water storage and filtration, flood reduction, wildlife habitat, biodiversity, and grazing (Lucas, 2016, p. 1). Given the numerous ecosystem services montane meadows provide, quantifying the impacts of climate change on California montane meadow systems is therefore essential for informing broader adaptive management goals that seek to mitigate climate change impacts on the region, and preserve the numerous ecosystem services these meadows provide. California, along with other Mediterranean biome regions, are predicted to experience a warmer and drier future (IPCC, 2013). As of 2000, spring advancement in California was three weeks earlier on average compared to historical records (Arnold, 2014, p.7). Determining how changes in water availability, timing, and rising temperatures impact vegetation productivity and community composition is an essential first step towards informing climate-adaptive planning and management strategies. Climate change itself has piqued interest in montane meadows in recent years, particularly in terms of their carbon sequestration and water storage. The former has garnered the attention of the California Air Resources Board (CARB) due to their potential of being incorporated into carbon markets established by A.B. 32 (CARB, 2015). Services such as water filtration and storage are

particularly important in the context of increasing drought incidence, motivating state agencies to enhance these services (CA Natural Resources Agency, 2016).

According to a 2013 study, most California mountain meadows are degraded, with 67% having been degraded by stream incision (Emmons, 2013, p. 25), causing a lower water table and drier soils, leading to vegetation community changes as conditions become too dry for typical meadow plants, as well as the species they support. Fish habitat is also impacted, with increased erosion decreasing habitat suitability (FR-CRM, 1996). Numerous restoration efforts are being undertaken in Sierra Nevada meadows, with the goal of restoring meadow vegetation and enhancing their ability to provide key ecosystem services. Restoration has been observed to increase meadow productivity, with a 25-50% increase in evapotranspiration after restoration (Lucas, 2016, p. 12). However, more work is needed across meadows that vary in their degree of degradation to better predict the capacity for restoration, and the overall effectiveness of restoration in the face of climate change. Observation thus far yields some conflicting messages as to how sensitive to drought and inter-annual precipitation meadows might be. One study found that vegetation in a Sierra Nevada meadow was not water limited, even during consecutive drought years (Lucas, 2016, p. 13). In contrast, a study in another Sierra meadow categorized as "pristine" found that drought did not only reduce productivity in the short term but can cause permanent damage to soils and vegetation, particularly if this exceeds historical drying maximums (Arnold, 2014, p. 64). Further, impacts on productivity varied in different hydrologic regions. Vegetation diverged in its response to snow cover timing and amount, with no significant change for dry areas, but a significant decrease in biomass in intermediate and wet areas (Arnold, 2014, p. 15). As such, questions remain as to how resilient meadow vegetation is

to drought conditions, how this varies among species and plant types, and how effective restoration might be in mitigating the impacts of more frequent drought.

1.3 Remote sensing to estimate productivity

Vegetation indices (VIs), typically derived from satellite imagery, are one of two ways to remotely estimate primary productivity. VIs have many applications, from use in crop and climate change modeling (Tempfli et al., 2009, p.149), to better understanding dynamics of phenology (Noumonvi et al., 2019; Yang et al., 2019). "Productivity" can be used to describe any number of terms, including net primary productivity (NPP), gross primary productivity (GPP), net ecosystem exchange (NEE), and aboveground biomass (AGB). Though they differ in terms of what aspects of ecosystem productivity they include (Chapin & Mooney, p. 97-119), any can be used in VI-based analyses. In comparison to physical mechanism models, which are the alternative method of quantifying productivity using remotely sensed data, VIs are the more popular option. This is because VIs can be used to estimate biomass in conjunction with relatively simple regression models, while requiring much fewer auxiliary data in comparison to physical mechanism models (Xu et al., 2021).

VIs are used to approximate productivity, being "proportionate to the amount of light energy absorbed by photosynthetic tissues", which also describes fraction of absorbed photosynthetically active radiation (fAPAR). VIs typically incorporates the reflective properties of chlorophyll in plants, which are highly reflective in near infrared (NIR). As such, higher VI values indicate higher levels of greenness. The most used VI, the normalized difference vegetation index (NDVI), which uses the formula below from Zhou et al., (2014):

$$NDVI = \frac{NIR - Red}{(NIR + Red)}$$

However, it can be a challenge to determine whether light is absorbed by soil, vegetation, water, etc. Further, plants differ in their reflectance in the visible range, making comparison between system difficult (Chapin & Mooney, p.118-119), with dense forests yielding much higher VI values than a sparse grassland. In addition to NDVI, numerous vegetation indices have been developed, with 21 indices being listed in a recent review by de Castro et al. (2021). The suitability of each VI will vary according to application, with vegetation type, scale, snow cover, soil types and visibility being some considerations.

1.4 Summary and project goals

There are many moving parts in the puzzle of changing water availability in grasslands and meadows. Changes in precipitation and temperature interact in complex ways that impact plant phenology and productivity. In some regions, changes in rainfall appear to increase productivity (Li et al., 2020). However, in the mountain meadows of California, projections of warmer, drier conditions are concerning particularly in areas where past land use history has resulted in degraded meadows. Despite this, restoration provides a means to improve the resiliency and function of these crucial ecosystems. To examine how a warming and drying climate impacts montane meadow biomass and community composition, further study is necessary to examine the relationship of water availability and meadow vegetation.

This work aims to improve the understanding of how montane meadow plant productivity and phenology varies in space and time in response to climate variability at several scales. A combination of remote sensing and field data was used to study the period between 2018-2021, to answer the following questions: (i) How does montane meadow plant phenology and productivity vary with climate variables, precipitation, and plant functional group during the

growing season? (ii) How does growing season duration and timing vary within and between years (2016-2021), and how does this variation relate to environmental drivers of plant water availability (i.e., snowpack, precipitation)?

2. Methods

2.1 Study area

Red Clover Valley (RCV) is a 2,655-acre (10.74 km^2) montane meadow in Plumas County, CA. It is located at an elevation of approximately 5,500 feet (1680 m), with the meadow itself being relatively flat. There are several creeks within the meadow, including Crocker and Dixie Creeks, which join to form Red Clover Creek (The Sierra Fund, 2018). It is an alluvial valley, with loam soils that range from fine-grained to gravelly (FR-CRM, 1996).

Like many meadows in the Sierra Nevada, RCV was degraded by various types of human activity, including overgrazing by cattle and beaver eradication, in addition to road and railroad construction, logging, and mining occurring within the broader 84 square mile (135 km^2) watershed (FR-CRM, 2008). Over time, the numerous creek beds became incised, resulting in a lowering of the water table associated with a decrease in mesic and hydric plant communities, and the proliferation of more xeric species such as sagebrush (*Artemisia* spp.). The large degree of erosion that resulted from the creek incision motivated the first restoration efforts in 1985, spanning 1 mile of stream length. This included the installation of check dams, revegetation, and cattle exclusion, alongside a commitment to monitor the effectiveness of restoration for 10 years. By 1996, several aspects of restoration had been successful, such as a significant rise of the water table, a return of mesic and hydric plants, and increased visitation of deer, waterfowl, and other bird species (FR-CRM, 1996). However, the check dams installed did not prove to be a suitable long-term solution to the site's erosion problems (Wild Fish Habitat Initiative, 2007), prompting further intervention, including plug and pond restoration methods along a larger span (3.5 mi.) of stream (FR-CRM., 2008).

Subsequent restoration projects have included other means of maintaining and enhancing previous efforts, incorporating rock grade control structures and beaver dam analogs, both implemented in 2018 (The Sierra Fund, 2018). The current project was launched in 2017, and is a collaboration between the Sierra Meadows Partnership, the Mountain Maidu, ranchers, and several universities. Field data collection efforts were in collaboration with several other entities to collect hydrology, vegetation, and wildlife data to inform goals to restore the meadow and increase habitat quality and availability. The meadow restoration project and concomitant monitoring efforts provide an opportunity to establish a baseline of species composition, seasonality, phenology, and productivity in this system, giving insight into the efficacy of restoration in the face of ongoing climate change.

2.2 Field data collection

The location and length of the field sampling transects were informed by an examination of NDVI images from the 2019 growing season, derived from 20 m Sentinel-2 data at the peak of the growing season. The location of the transect displayed a variation in NDVI values, hypothesized to be linked with the existence of a hydrologic gradient, with vegetation greenness being a bioindicator of variable water availability in the meadow. Though the meadow is relatively flat, proximity to streams and topographical features impacts water availability throughout the study area. The South and East transects coincide with wetter areas, closer to several streams that are the result of water diversion. The North and West transects were in drier areas, without as much influence from streams, particularly farther from the center (Figure 1).

Figure 1. Sampling locations in Red Clover Valley

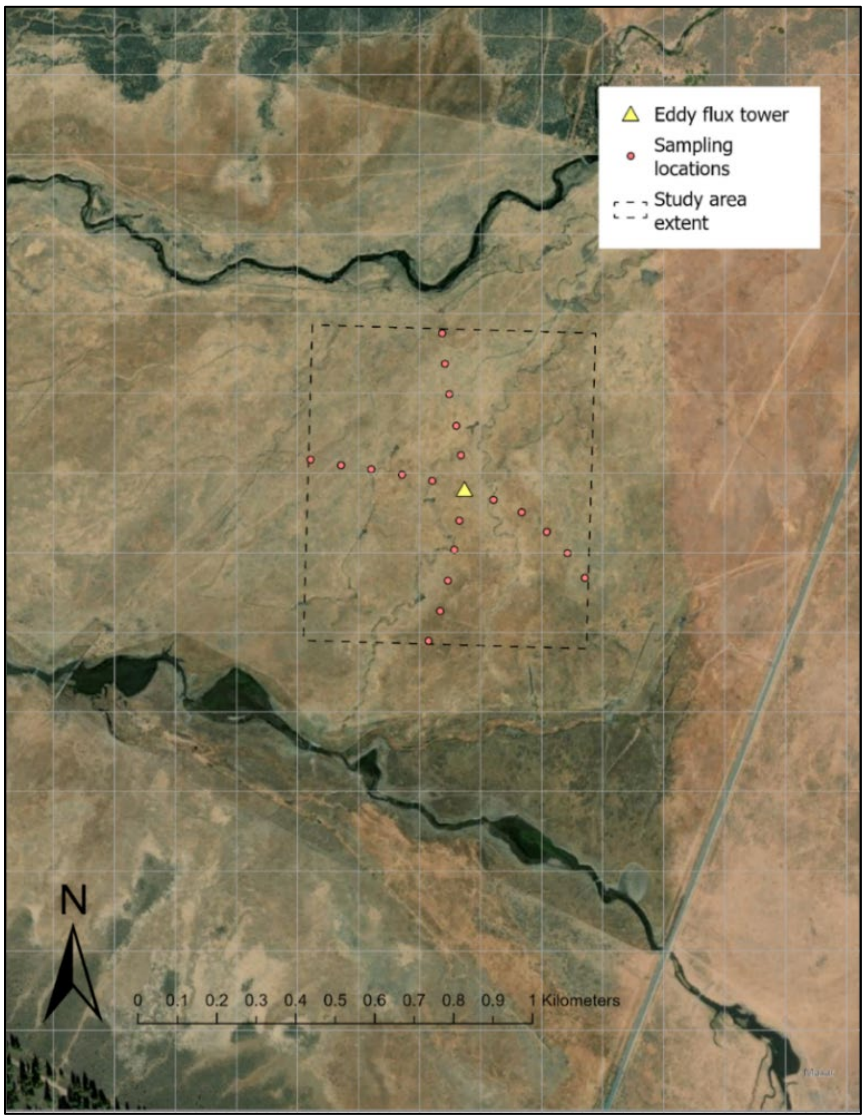

Figure 1. Field data was collected from each of the sampling locations (red). Remote sensing analysis sampled these points, in addition to the entire study area (dotted line).

The four transects radiated in each of the cardinal directions from the eddy covariance tower, which provided continuous measurements of micrometeorological variables, carbon flux, water vapor flux, and soil moisture at a single point location at depths of 10, 20, 50, and 100 cm. The length of the transects (300 m), was chosen to span an area that showed considerable variation based on 2019 NDVI data. To ensure that only one plot fell within each 10 m pixel, the

20 sampling locations were spaced 60 m apart. Sampling locations were georeferenced using a Trimble R1 GPS Receiver, which provides submeter accuracy, in conjunction with the GNSS Status mobile application (Trimble, Inc. Version 3.0.8.673). Points were recorded using the ArcGIS Collector mobile application (Version 21.0.4).

Field sampling dates took place throughout the growing season, on a roughly monthly basis: 6/2 (DOY 153), 6/28 (DOY 179), and 8/3 (DOY 215). From each of the 20 plots, samples were collected for aboveground biomass, plant water content, shallow soil moisture (0-10 and 10-20 cm), and belowground biomass (only 8/3). Following the 6/2 sampling, measurements were made in plots 1 m to the right of the previously sampled plots that had similar plant community composition.

Aboveground biomass (AGB) was harvested by clipping all plant material (living and dead) within a 0.25 m^2 quadrat. The total wet weight of the plant material was measured immediately after clipping using Pesola field scales (100 g and 500 g). A soil moisture probe (FieldScout, TDR 150 Soil Moisture Meter) was also used to measure shallow (0-10 cm) soil moisture at each plot. In early August, belowground biomass was also collected using a soil auger to a depth of approximately 30 cm.

AGB samples were collected within a 2 to 3-hour window in the morning to minimize the wilting of plant samples. Leaves needed to be scanned as soon as possible after collection, as a loss of turgidity could lead to an underestimation of leaf area, particularly with herbs. To mitigate this, samples were stored in a cooler, and damp paper towels were added to each bag of samples. On 6/2, samples were placed in a cooler with dry ice soon after sampling (1-3 hours).

On later sampling dates, a portable cooler was used, and samples were put on ice and/or ice packs at the time of collection.

After collection, photosynthetic (green) plants were sorted into three plant functional groups (PFGs) in order provide a rough sketch of changing community composition and productivity over the growing season. The plant functional groups used included rush, sedge/grass, and herb, represent different responses to water availability and drought, resulting from different plant traits (rooting depth, leaf area, drought tolerance, et cetera). Senesced plant material was separated out and labeled as standing dead. The standing dead (SD) category was not separated further into PFGs due to the difficulty of discerning differences of dry, withered plants with similar physiology (i.e., withered rushes vs. sedge/grass). However, composition of SD appeared to reflect overall species composition observed in the data collected. Green leaf area (LA) was also measured using a tabletop scanner (LiCor, LI-3100C). The leaf area of each PFG was used to calculate the percent cover of each group. The dry weight was recorded by PFG for each plot (Cole-Palmer, P-bal HC 1kg x 0.01g IntCal), after drying samples at 100 °C for 24 hours (Fisher Scientific, 100L GP gravity oven). A similar method was used for belowground biomass samples. After soil was removed from the roots, samples were sieved, then rinsed in a tub of water. After washing, samples were allowed to dry at room temperature, then weighed after being dried at 100 °C for 24 hours.

Additional datasets used from the meadow include predawn water potential, a measure of plant water status, using a Scholander Pressure Chamber. Leaf vapor pressure deficit, and climate and soil data (0-100 cm), monitored continuously at the eddy flux tower (EFT). Predawn water potential and stomatal conductance measurements were collected on 6/2 and 6/28. For

predawn water potential of a plot, samples were taken by plant functional group and were then weighted by each group's relative contribution to cover. Climate and soil data (0-100 cm) were monitored continuously at the eddy flux tower (EFT) (Figure 1).

Metrics calculated from field data included aboveground biomass per unit ground area (AGB), leaf area index (LAI), plant water content (PWC), and the roots-to-shoots (R:S) ratio. Formulas used to calculate each are listed below:

$$AGB\ (\frac{g}{m^2}) = \frac{Plot\ dry\ weight\ (g)}{Plot\ area\ (m^2)}$$

$$LAI = \frac{Leaf\ area\ (m^2)}{Plot\ area\ (m^2)}$$

$$PWC\ (\%) = \frac{Wet\ weight\ (g)\ -\ Dry\ weight\ (g)}{Dry\ weight\ (g)} \times 100$$

The root-to-shoot ratio (R:S) is ratio between the dry weight of aboveground and belowground material (Harris, 1992), and is used to indicate the proportion of root to leaf allocation. Statistical analyses, including linear models and ANOVA tests, were conducted in RStudio, using R (Version 4.1.1) or Microsoft Excel (Version 2108).

2.3 Remote sensing data

2.3.1 VI selection

With an average of 240.48 g/m² in the 2021 growing season (Figure 2A), the meadow vegetation in 2021 was not "dense" according to the threshold of 300 g/m² (Xu et al., 2021), necessitating a VI that accounts for bare soil. Additionally, this means that VI saturation should not be a large source of error, as there are no evergreens present in the study site (which could contaminate the signal and introduce error), and the latitude is less than 55°N, VIs should be able to detect green-up more easily (Cao et al., 2020). One source of error that needs to be assessed is

how rapidly green-up occurs. In a study where this green-up occurred a month after snowmelt, VIs were able to detect this change, as it was sufficiently slow. In Red Clover Valley, eddy covariance tower data indicates that green-up occurred in early April, with the system becoming a C sink some 20 days later (Martin et al., 2021). As snow persisted into April at the nearby Portola, CA weather station (NowData, NWS), it seems like green-up was rapid in the 2021 growing season, possibly occurring concurrently with snowmelt.

Given the consistent presence of winter snow in the study area, in addition to the relatively high performance of these indices in similar ecosystems, a VI which takes into account snow cover should be used, and of those reviewed, the normalized difference phenology index (NDPI) and normalized difference greenness index (NDGI) are most suitable. However, in comparison to NDPI, NDGI was developed specifically to be able to differentiate dead from living matter, important in sites with substantial amounts of standing dead biomass. As demonstrated by plant cover estimates (Figure 2a), standing dead was dominant during much of the sampling period, taking place from 6/2 to 8/3. In contrast, NDPI was seen to outperform NDGI in its ability to suppress the soil background, though other studies found that this may be less important at the field scale (at which the current study is conducted), compared to the region scale studied in Cao et al. (2020). In Red Clover Valley, the presence of bare soil was recorded at the time of sampling, with some bare soil present at 7 of 20 sites in the most productive part of the growing season. As there was an apparent absence of leaf litter from the previous season, this may indicate that these areas of bare soil may be persistent. This, in addition to the relatively sparse vegetation means that a VI that accounts for bare soil is necessary.

In addition to distinguishing dry vegetation, NDGI has the additional advantage of being more easily applied to more data sources than NDPI, which was developed for MODIS data and uses the SWIR band, which further narrows which data sources can be used. In contrast, NDGI can be used for any satellite so long as the formula is edited to reflect satellite parameters, and only uses the green, red, and NIR bands (Yang et al., 2019). The formulas are as follows:

$$NDGI\ (MODIS) = \frac{0.65\ \times green + 0.35\ \times NIR - red}{0.65\ \times green + 0.35\ \times NIR + red}$$

$$NDPI = \frac{\text{NIR} - (0.74\ \times\ red\ +\ 0.26\ \times\ SWIR)}{\text{NIR}\ +\ (0.74\ \times\ red\ +\ 0.26\ \times\ SWIR}$$

A threshold based on the results of the NDGI analysis was used to delineate the tail ends of the growing season. The use of relative VI thresholds is one method of estimating the beginning and end of the growing season (Yang et al, 2019). As the NDGI did not reach zero even when the vast majority of vegetation was dormant, an NDGI of 0.05 was used as a threshold of when the meadow was no longer productive, signaling the beginning or end of the growing season.

2.3.2 Workflow

Sentinel-2 imagery at 10 m resolution was acquired either from Copernicus SciHub (https://scihub.copernicus.eu/). For dates after 2019, level 2A images were available, which are atmospherically corrected bottom-of-atmosphere (BOA) images. For dates prior to 2019, additional steps were required to convert them from level 1C top-of-atmosphere (TOA) to level 2A BOA images. The European Space Agency's (ESA) SNAP application (Version 8.00) was used to utilize the Sen2Cor tool (Version 2.10.01). This process is used by ESA when converting images from 1C (TOA) to 2B (BOA), using scene classification to create a probabilistic cloud mask to identify and remove clouds, cloud shadows, etc. from the image (Sen2Cor Configuration

and User Manual, 2021). Full images were cropped to the extent of the study area and composited in ArcPro (Version 2.9.2) using a Python script. These images were then used to calculate NDGI for each image, using a Python script utilizing the formula below, with satellite parameters calculated for Sentinel-2 sensor 2A.

$$NDGI\ (\text{Sentinel-2A}) = \frac{0.616 \times Green\ +\ 0.384 \times NIR\ -\ Red}{0.616 \times Green\ +\ 0.384 \times NIR\ +\ Red}$$

After the NDGI was calculated for the entire image, it was also extracted for the extent of the sampling area and for each sampling site (Figure 1). To obtain values for the extent of the study area, the raster was exported, with the extent set to the bounds of the field sampling transects. The "Sample" tool was used to extract the values at each of the sampling locations.

3. Results

3.1 Community composition and productivity in the 2021 growing season

Though sedge and grass (SG) was the dominant PFG throughout the season based on percent cover, community composition shifted throughout the growing season, both in terms of photosynthetic and standing dead (SD) plants (Figure 2). Standing dead biomass was a substantial portion of total cover by 6/2 (~32%), increasing significantly by 6/28 (to ~70%), with a more modest increase by August 3 (to ~77%). In terms of photosynthetic plant cover, the contribution of SG to total cover increased as the season progressed.

Figure 2. Community composition on 2021 sampling dates

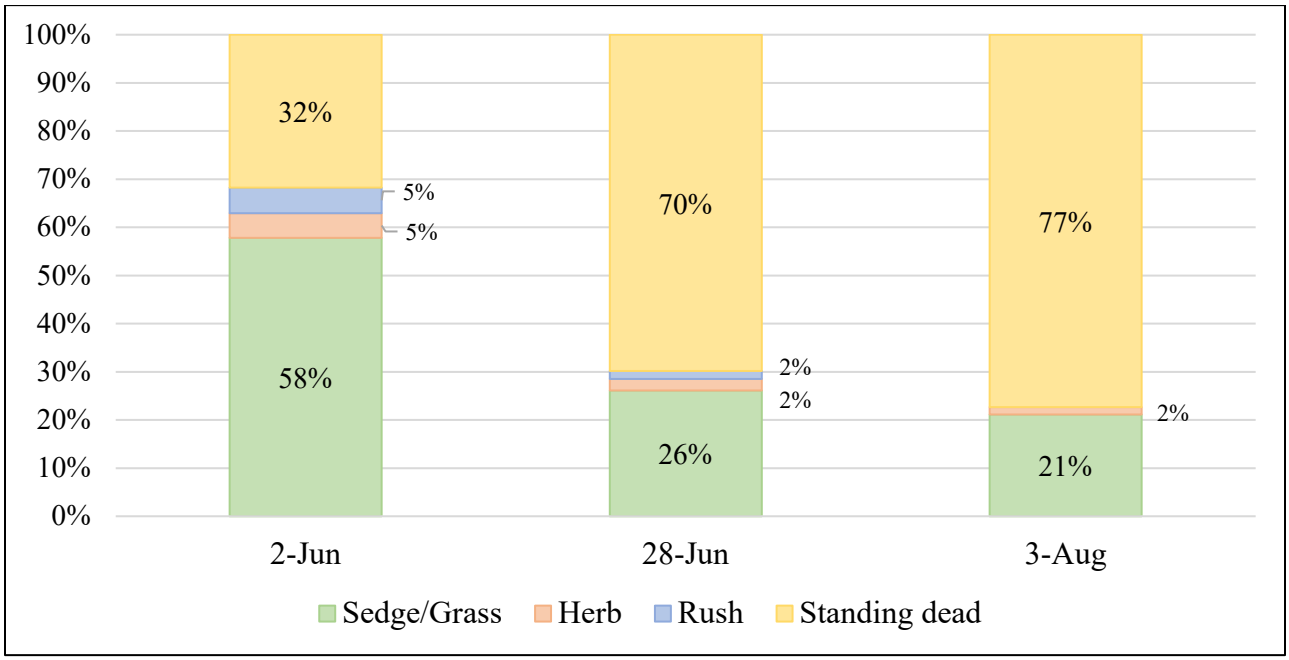

Figure 2. Contribution of each plant functional group to total cover. Cover calculated from the leaf area of each plant functional group and pooled for all plots by sampling date.

Rushes (R) decreased by 75% between early and late June, ultimately disappearing by the 8/3 sampling date. Herbs (H) increased by 14% between 6/2 and 6/28, and decreased to 11% of total cover by 8/3, a more modest 21% decrease from 6/2.

Plant dry weight decreased significantly between sampling dates, with the biggest difference observed in SG (Figure 2). There was a significant difference between the dry weight of SG and the other PFGs, but the difference between H and R was not significant. Between 6/2 and 6/28, 54% of the variation in dry weight could be explained by PFG and DOY, though this dropped to 42% with the inclusion of the 8/3 data ($p = 0.0002$), implying that other factors became more important as the growing season progressed (Appendix C). In addition, this varied between PFGs, with variation in dry weight through time only being significant for SG, for which it was highly significant. For SG only, the interaction between PFG and DOY was also significant ($p = 0.0062$) (Appendix C).

Figure 3. Average aboveground biomass on each sampling date

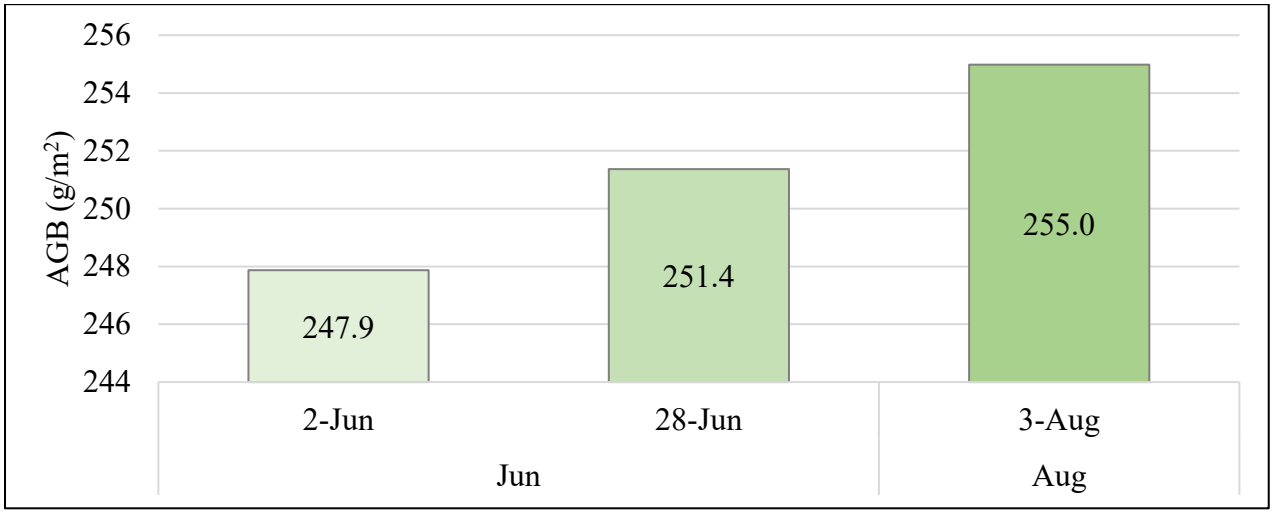

Average aboveground biomass per unit ground area (AGB), (Figure 3), showed a modest increase between sampling dates (Figure 3). AGB accumulation may have been decreased

overall due to grasshopper herbivory, a large swarm being present on the site at 6/28 (Personal observation). Overall, average AGB increased just 3% between 6/2 and 8/3, indicating that the peak of the growing season occurred near or prior to 6/2.

The difference in average soil moisture (SM) for all plots at 0-10 cm showed highly significant differences between sampling dates ($p < 0.001$). In the early season, there was a much larger range in soil moisture (9.5-65.2% VWC) (Figure 4), which decreased as the season progressed, ranging between 5.5-29.4% by 6/28 and 3-17.2% by 8/3.

Figure 4. Boxplots of soil moisture (10 cm) on each sampling date

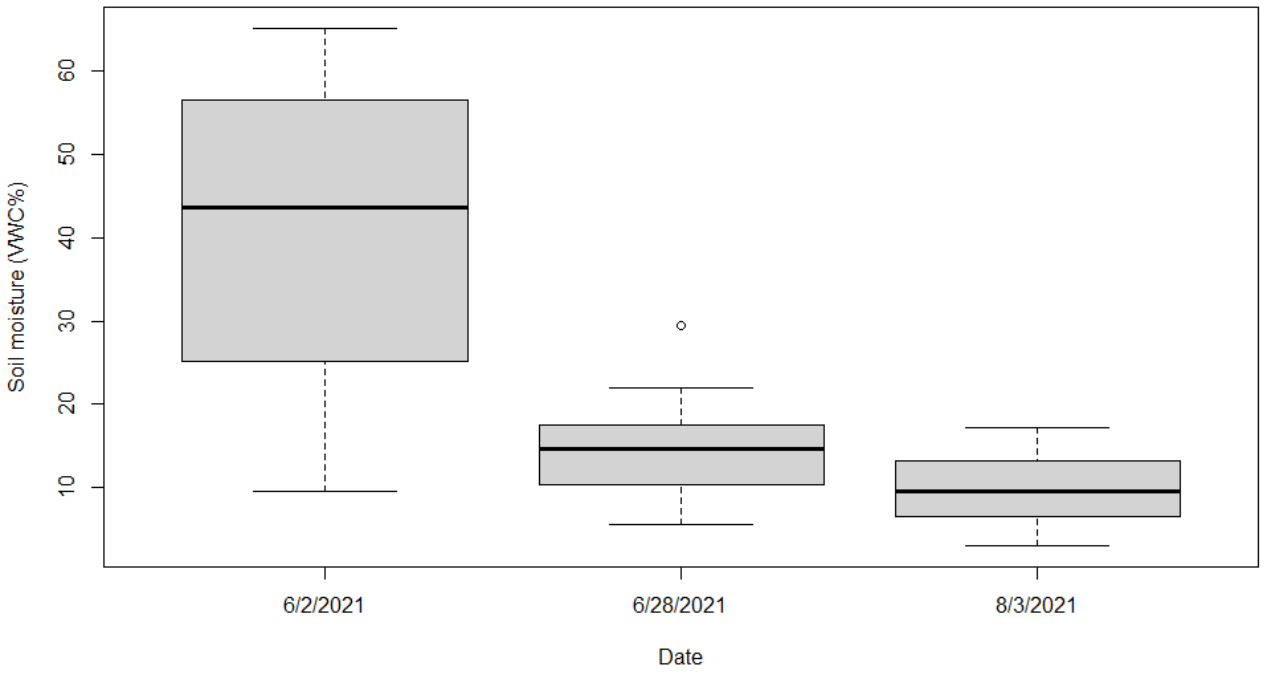

Earlier in the season, there were significant differences in the soil moisture between the four transects, though values converged as the meadow dried and senesced (Figure 5). In the earlier part of the growing season, there was a significant difference between the South (wettest) and all other transects. On 6/28, there was a significant difference between the North (driest) and

South (wettest) transects. By early August, there was a very slight significant difference between transects (Table 1).

Figure 5. Soil moisture by transect on sampling dates

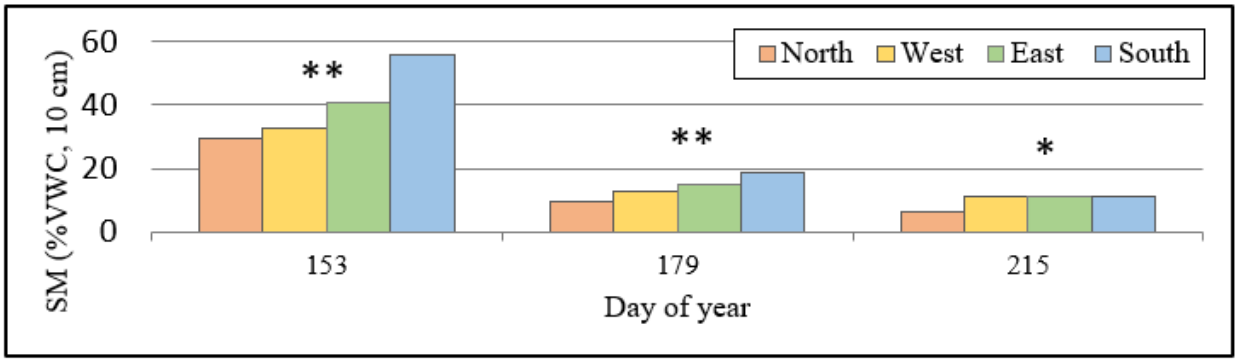

Figure 5. Asterisks indicate significant difference between transects, generated with ANOVA tests for each sampling date.

Table 1. Differences in soil moisture (VWC%) by transect

DOY	p-value	Notes
153	0.0018	S significantly different from all transects
179	0.0025	S/N are significantly different
215	0.048	Slightly significant difference

Table 1. P-values were from ANOVA tests for each sampling date. Notes are from ANOVA tests used to compare differences each between individual transect.

In examining relationships between dry weight, soil moisture, and PFG, SG was the only PFG significantly impacted by shallow soil moisture (Figure 6), with the interaction between PFG and soil moisture being more significant ($p = 0.001$) than PFG alone ($p = 0.031$) (Appendix C). Shallow soil moisture was not associated with a significant difference of dry weight in H or R, but was highly significant but weakly related for SG, with SM (0-10 cm) accounting for 21% of variation in dry weight for SG.

Figure 6. Relationship between soil moisture and dry weight by PFG

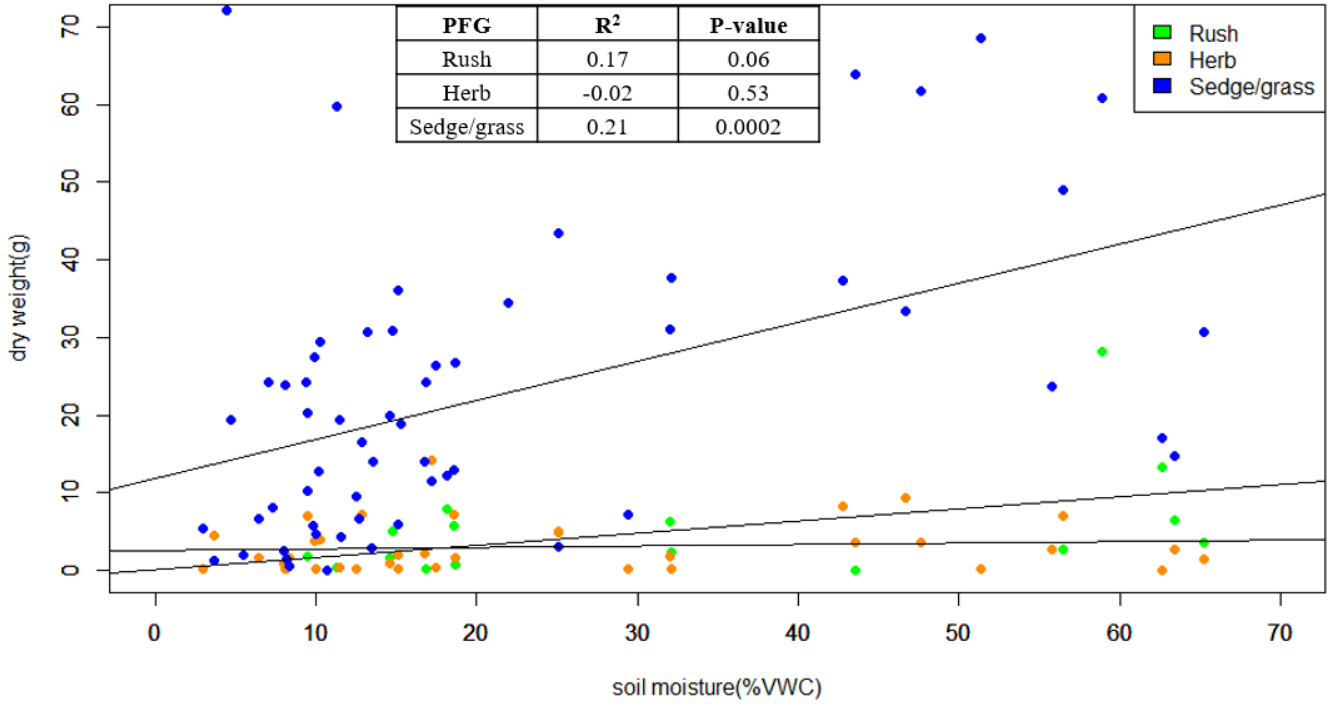

Leaf area (LA) and leaf area index (LAI) were highest on 6/2, with LAI decreasing 54% between 6/2 and 6/28, then 13% between 6/28 and 8/3. DOY and PFG were significant for the leaf area of SG, but not H or R. This can be seen in the precipitous decrease in SG leaf area between DOY 153 and 179 (Figure 7), with a decrease of ~46% in leaf area between those dates. For the leaf area of SG, PFG, date, and their interactions were both highly significant and explained 50% of the variation in SG leaf area ($p < 0.001$). Similarly, the interaction between soil moisture and PFG was highly significant for the leaf area of SG ($p < 0.001$), accounting for 48% of variation (Appendix C).

Figure 7. Leaf area and PFG in the 2021 growing season

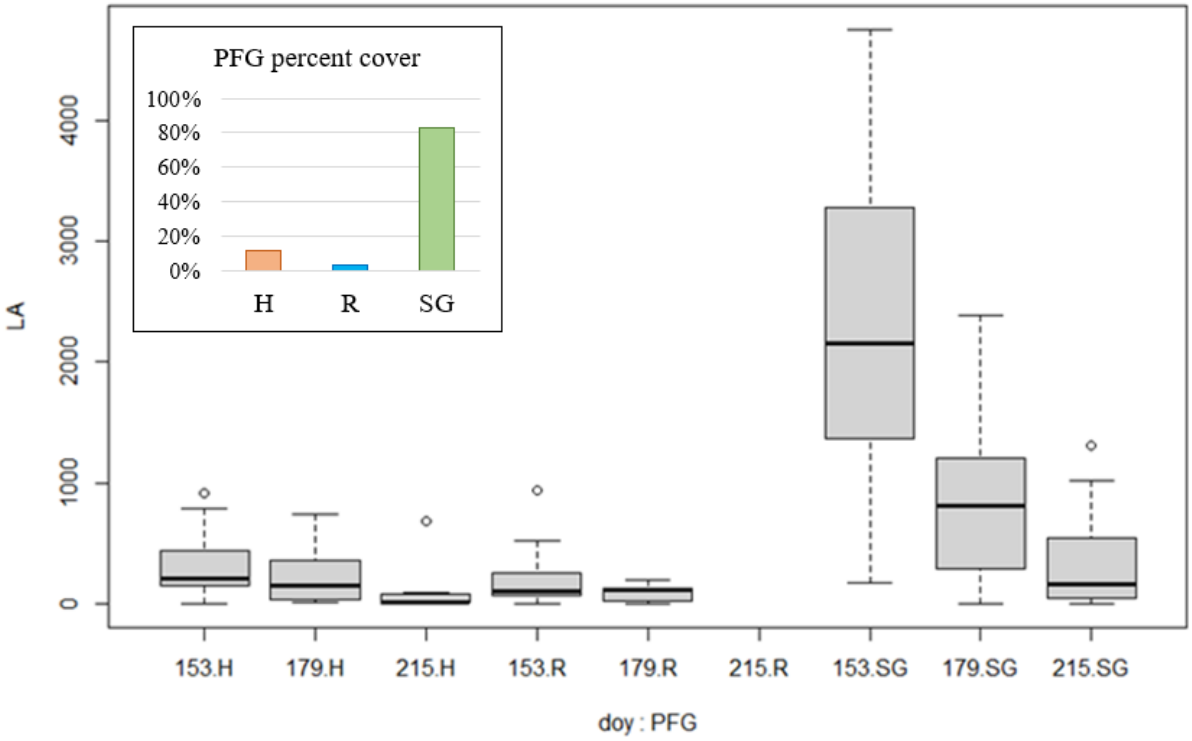

Figure 7. PFG percent cover (top left) reflects each plant functional group's contribution to total photosynthetic cover, averaged across all plots and dates.

Belowground biomass (BGB) was collected on 8/3. The R:S from 8/3 shows a relatively low allocation of energy to roots (Figure 8a), with most values occurring between 0.00-0.15, with just 2 instances of roots reaching over one third of corresponding leaf mass. BGB values were not significantly different between transects, though there was a slightly significant difference between R:S of the West and East transects ($p = 0.055$), the former having a higher median as well as more variation than the latter (Figure 8b). BGB harvested on 8/3 also did not have a strong relationship with dry or wet weight, or leaf area.

Figure 8. Roots allocation at sampling locations

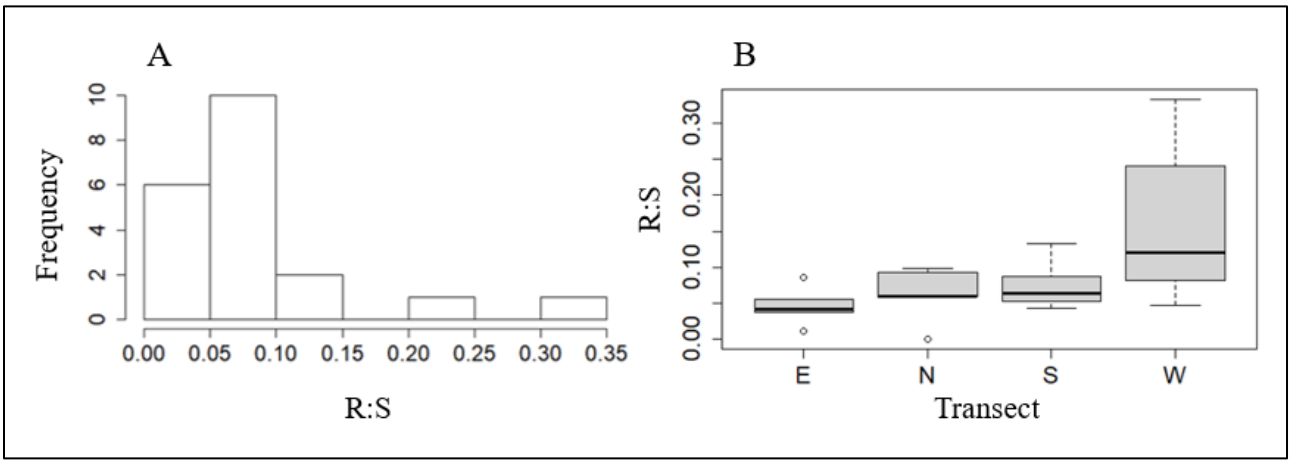

Figure 8. a) Histogram of root-to-shoot ratio for all sampling locations on 8/3. b) Boxplots of root-to-shoot ratio by sampling transect.

Predawn water potential, sampled on 6/2 and 6/28, was a good predictor of plant water content throughout the growing season ($R^2 = 0.55$; Figure 9). Values of predawn water potential closer to zero indicate higher plant water status. Low soil moisture values at 0-10 cm in the later growing season correlates with lower plant water status (Figure 9). This indicates that plants were obtaining water from deeper than 0-10 cm, supported with soil moisture data collected between 0-100 cm at the EFT, which showed that water at depths of 0-20 cm disappeared between DOY 180 and 200. Though this is just one sampling point, soil moisture data at plots (0-10 cm) was well-correlated to EFT data at same depth ($R^2 = 0.57$). In addition, shallow SM collected at plots were also not strongly correlated to predawn water potential ($R^2 = 0.13$; Appendix C).

Figure 9. Pre-dawn water potential and plant water content

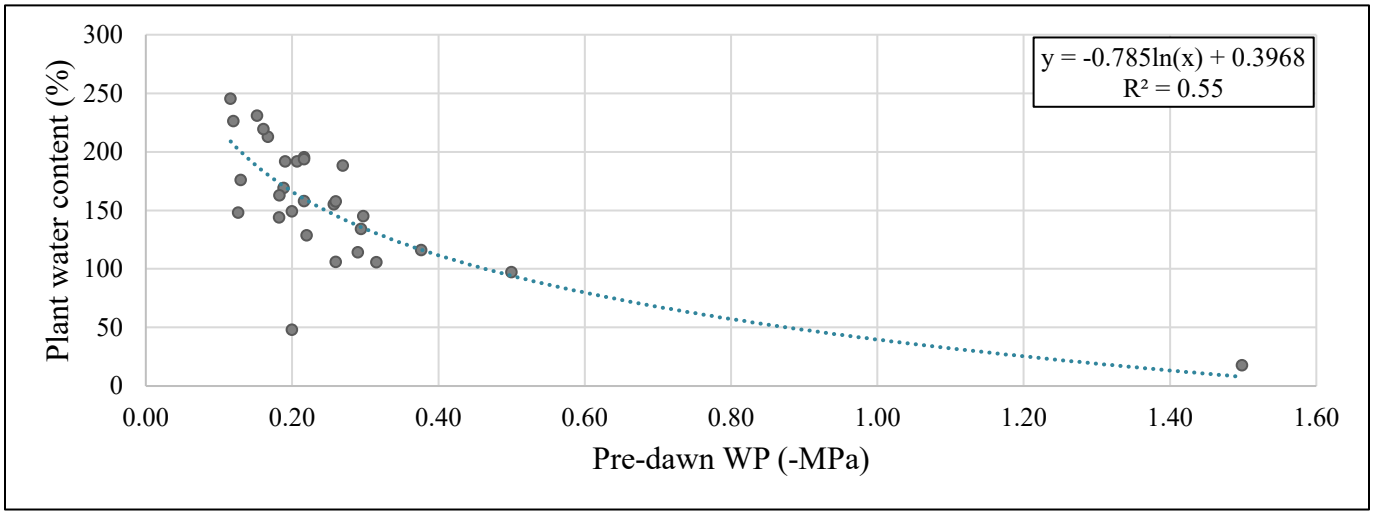

Figure 9. Points represent plant water content and predawn water potential, with all plant functional groups were combined after being weighted by their contribution to total community composition.

As plants remained photosynthetic past DOY 200, this points to plants obtaining water from deeper horizons. However, the relationship between soil moisture and plant water content (PWC) decreased in strength and significance with depth, no longer being significant at 100 cm, indicating that most of the plant available water was between 0-50 cm, and mostly between 0-20 cm.

Table 2. Correlations between soil moisture and plant water content

Depth	Correlation (R^2)	Significance (P-value)
10 cm	17.1%	0.0009
20 cm	16.6%	0.001
50 cm	9.6%	0.01
100 cm	0.0065%	0.25

Table 2. Soil moisture values were measured continuously at the EFT. Plant water content data was collected from different plant functional groups at the plot level.

Figure 10. Leaf vapor pressure deficit and stomatal conductance

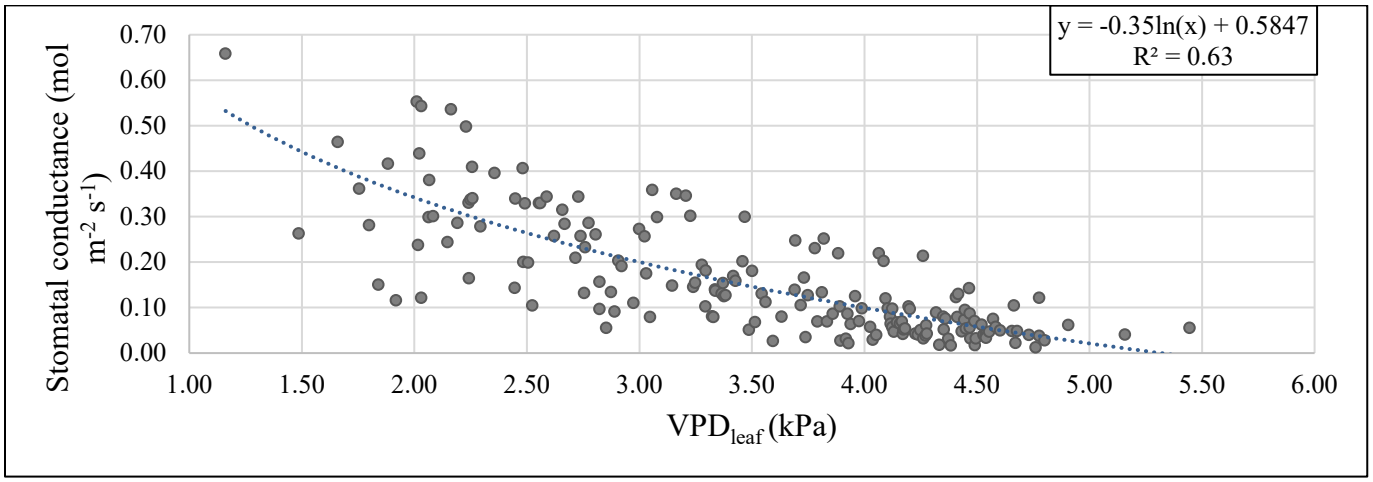

Stomatal conductance was inversely related to leaf vapor pressure deficit (VPD_L) across PFGs regardless of plant water status (Figure 10). The relationship between stomatal conductance and VPD_L show that high VPD_L limited productivity, even during periods of higher water availability. This suggests that VPD is an important control of stomatal conductance and plant productivity over the growing season. This is supported with EFT data, which showed that maximum VPD was a highly significant predictor of PWC ($R^2 = 0.18$, $p < 0.001$), also displaying an inverse relationship.

3.2 NDGI Analysis 2018-2021

3.2.1 Study area extent NDGI

Based on the results of the NDGI analysis for the extent of the entire 600 m^2 study area, which formed a square around the transects (Figure 1). 2021 had the shortest growing season of all years 2018-2021. In 2021, average NDGI remained above the threshold of 0.05 for just 3-4 months, from April or May until July. In 2018, 2019, and 2020, NDGI remained at or above 0.05 for approximately 5-6 months, from April until late August/September (Figure 11). The 2021

peak was also the lowest between 2018-2021, with a mean NDGI of 0.32 on 6/2, 2021. For comparison, this was 0.41 in 2018, 0.52 in 2019, and 0.59 in 2020.

Figure 11. NDGI of 600 m^2 study area extent

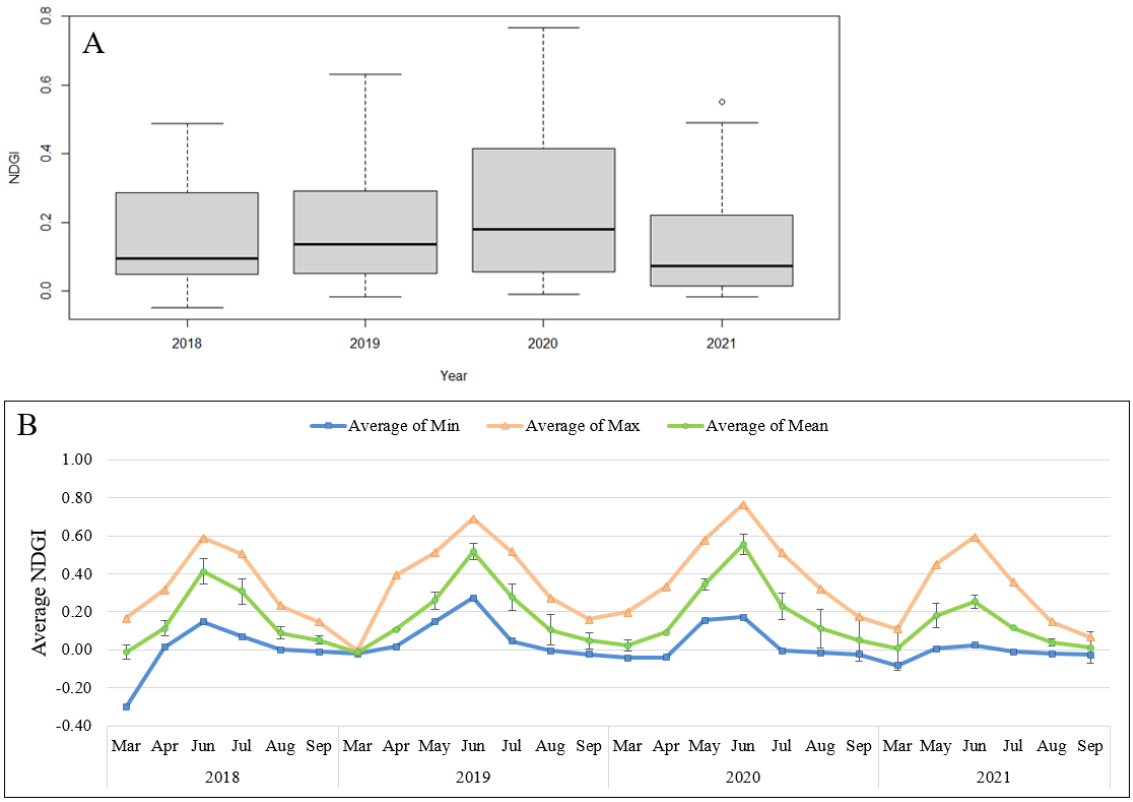

Figure 11. a) Represents median and range of NDGI values for 2018-2021, from all pixels within the extent of the sampling transects. b) Average min, max, mean, and standard deviation of NDGI from 2018-2021 of all pixels within the extent of the sampling transects.

The average mean and max NDGI indicate that 2020 was the most productive growing season, with an overall mean NGDI of 0.25 and an average max of 0.46 (Table 3), compared to 2019 (mean=0.19, max=0.36) and 2018 (mean=0.16, max=0.33). Both 2020 and 2021 markedly higher average standard deviation compared to 2019 and 2018 (~0.07 vs. ~0.04 average standard

deviation). This implies a greater degree of variation, which could be attributed to several different factors, such as differences in community composition and thus differences of plant response to water availability.

Table 3. NDGI values of 600 m^2 study extent **(**2018-2021)

Year	Avg. min.	Avg. max.	Avg. mean	Avg. std. dev.	Peak date	Avg. peak NDGI
2018	-0.01	0.33	0.16	0.04	6/14	0.41
2019	0.06	0.36	0.19	0.05	6/19	0.52
2020	0.05	0.46	0.25	0.07	6/8	0.59
2021	-0.01	0.33	0.12	0.07	6/3	0.32
Overall avg.	**0.02**	**0.37**	**0.18**	**0.06**	**6/11**	**0.46**

When comparing the study area NDGI to the entire meadow extent, which utilized a mask to exclude the surrounding forest, some slightly different patterns emerge. The NDGI for the entire meadow extent was well-correlated to values at the plot ($R^2 = 0.76$) and study area ($R^2 = 0.84$). Though 2021 remains the year with the lowest peak NDGI values, 2018, 2019, and 2020 are much more similar, with peak average NDGI ranging from 0.2442 to 0.2726. Like NDGI in the study area, the peak occurred in early- or mid-June. However, for the entire meadow extent, the highest mean peak NDGI was in 2019, versus 2020 in the study area, also corresponding to the year with the highest precipitation. In comparison to the study area, the extent of the meadow had markedly lower peak NDGI values than the study area, which supports the assumption that the transects spanned a more hydric area. In addition to higher peaks, NDGI values in the study area were also slightly lower compared to the entire meadow, which is also consistent with the

presence of a more hydric vegetation community being less productive in the drier part of the growing season.

Figure 12. NDGI of meadow extent and study area

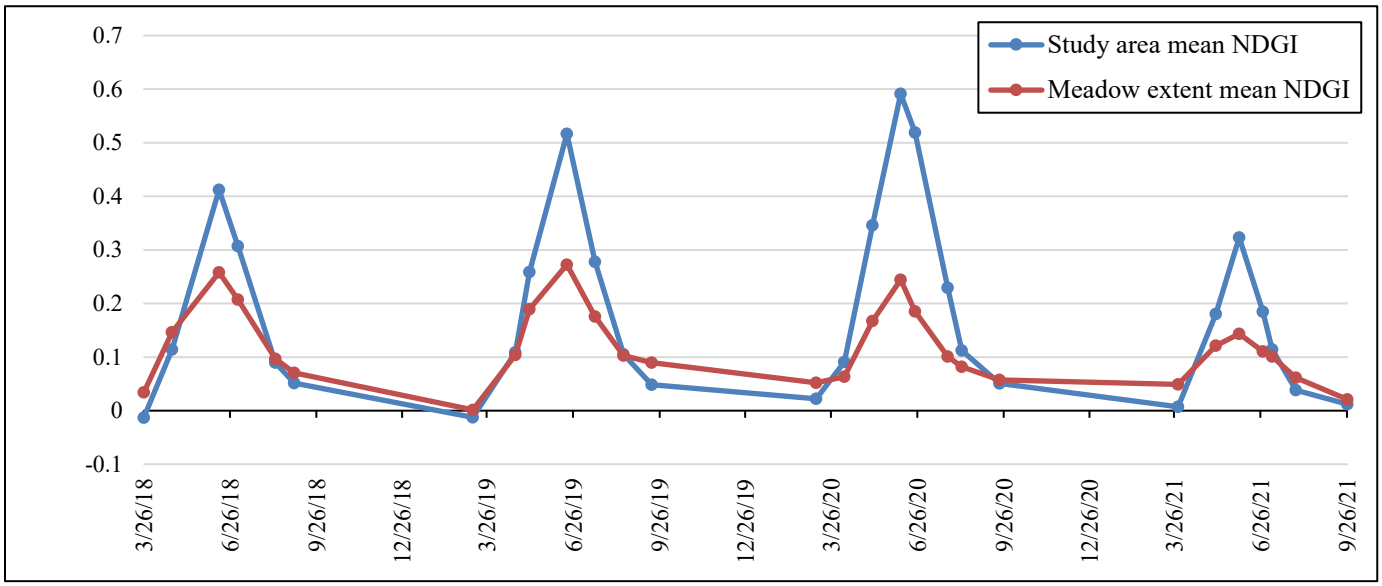

3.2.2 Plot-level NDGI

The average NDGI at the plot level (Figure 13a) were very well-correlated to the whole meadow extent ($R^2 = 0.84$; Appendix C) and study area ($R^2 = 0.899$) but allowed for additional insight into patterns by individual plot and transect. The North transect had the highest NDGI at the start of the 2021 sampling period (Figure 13b), despite being the driest transect in terms of shallow SM. The smallest decrease in NDGI throughout the season was seen in the South transect, which also experiences a smaller decrease in soil moisture compared to the others. Despite these differences, the relationship between NDGI and plot/transect was not significant during the 2018-2021 study period.

Figure 13. Plot-level NDGI 2018-2021

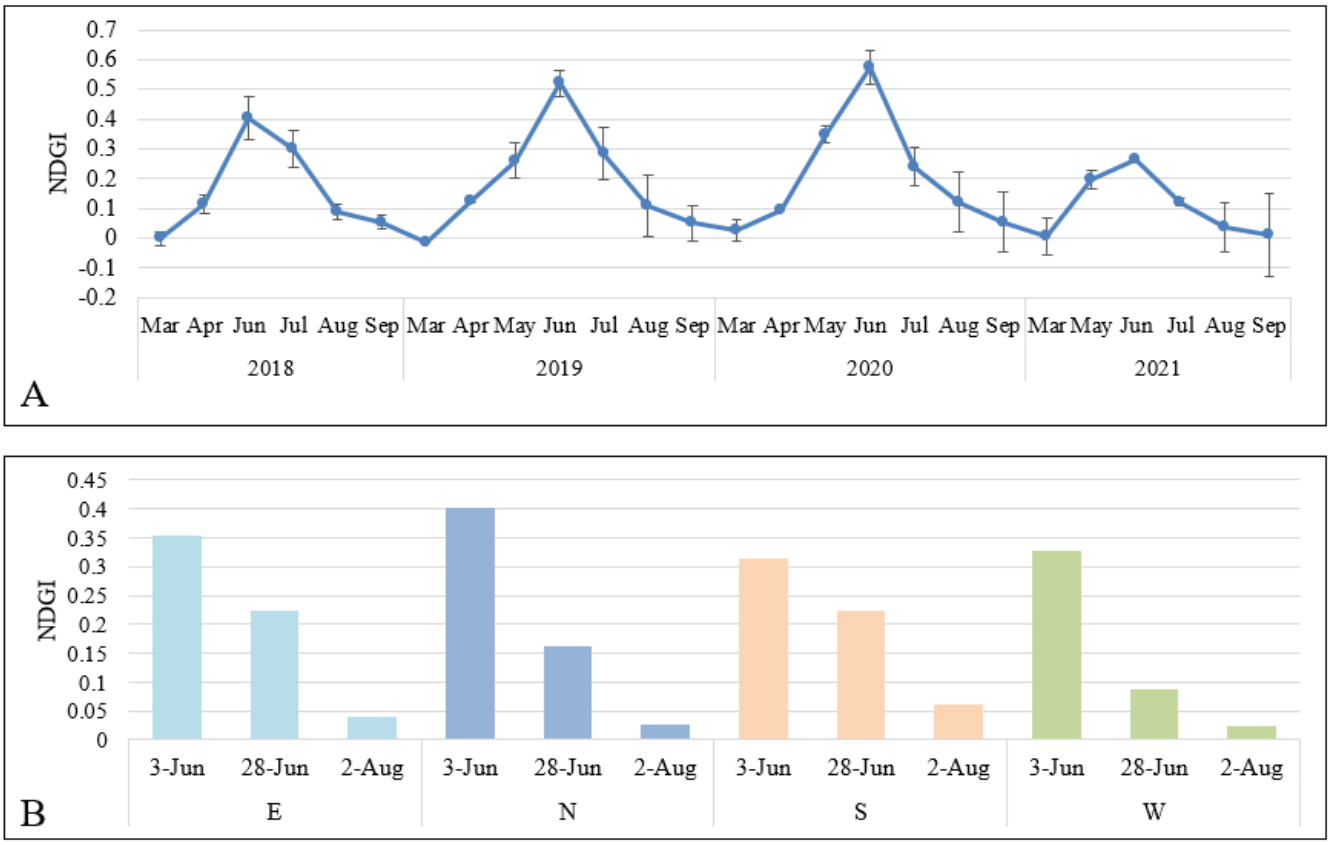

Figure 13. a) Average NDGI from 2018-2021 at the plot level for all the 20 sampling areas. b) Average NDGI of each transect on each sampling date from the 2021 growing season.

3.2.3 Correlations between NDGI and field data

Of the productivity measurments collected in the field (AGB, dry and fresh weight), the average NDGI was most closely correlated to the average fresh weight ($R^2 = 0.97$) for the dates sampled in the 2021 growing season. There was no correlation between NDGI and AGB ($R^2 = 0.03$) or average dry weight ($R^2 = 0.0019$) (Figure 14), which is expected given that NDGI is responding to greenness of vegetation, and thus would not correlate well with dead vegetation. However, when using all fresh weight data for the sampling dates (vs. the average), the R^2

decreased from 0.97 to 0.40 (Table 4). The correlation also varied in strength throughout the growing season. When analyzed by sampling date, the relationship between NDGI and fresh weight was significant on 6/2 ($p = 0.005$, $R^2 = 0.33$) and 6/28 ($p = 0.0018$, $R^2 = 0.40$), but not on 8/3 ($p = 0.36$, $R^2 = -0.006$). For AGB and dry weight, the strength of the relationship remained low throughout the growing season. The correlation between LAI and NDGI was also strong and highly significant when including all sampling dates ($R^2 = 0.59$, $p < 0.001$; Figure 14). Looking at the data by date, the relationship between LAI and NDGI decreased alongside increasing amounts of standing dead vegetation (Table 4), being somewhat significant on both 6/2 ($R^2 = 0.17$, $p = 0.04$) and 6/28 ($R^2 = 0.20$, $p = 0.026$). By 8/3, there was no significant relationship between the two ($R^2 = 0.07$, $p = 0.14$).

Figure 14. Relationships between NDGI and fresh weight, PWC, and LAI

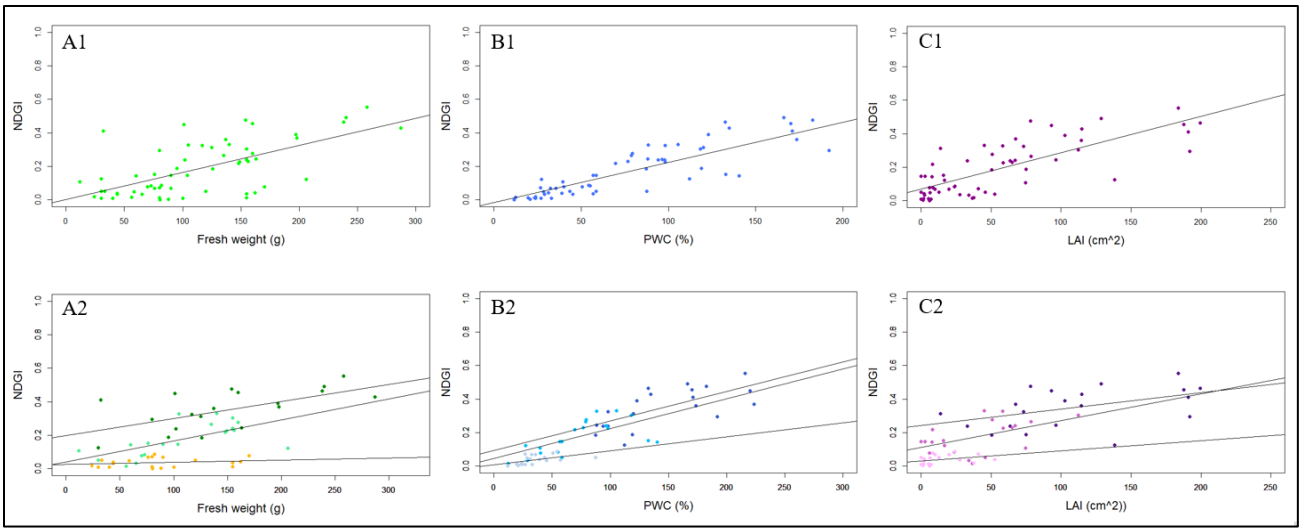

The relationship between plant water content (PWC) and NDGI was highly significant having the highest correlation with NDGI overall ($R^2 = 0.7651$, $p < 0.001$). Like other factors, this

relationship varied in strength throughout the growing season (Table 4), being significant on June 2 ($R^2 = 0.43$) and June 28 ($R^2 = 0.37$), then somewhat significant on August 3 ($R^2 = 0.24$).

Table 4. Correlation between NDGI and fresh weight, PWC, and LAI

Variable	R^2 (6/2)	R^2 (6/28)	R^2 (8/3)	Overall R^2
Fresh weight	0.33	0.40	-0.006	0.40
PWC	0.43	0.37	0.24	0.77
LAI	0.17	0.20	0.07	0.59

In addition to the strong relationship of PWC to NDGI at the plot scale, PWC was significantly related to both CO_2 ($p = 0.008$) and H_2O fluxes ($p = 0.0014$) based on chamber data from 6/2 and 8/3, explaining 16% to 24% of variation, respectively (Appendix C). In conjunction, CO_2 and H_2O fluxes were highly correlated, with H_2O fluxes explaining 64% of the variation in C fluxes ($p = p < 0.001$), making H_2O fluxes a good proxy for C fluxes in the meadow (Appendix C).

3.3 Plumas County climate 2018-2021

Based on the monthly Sentinel-2 images, the difference in snow presence between years ranged from 200-242 days (Table 5). Snow melt was detected latest in 2019 (7/21), and earliest in 2021 (6/5). Though 2020 had the most productive growing season based on NDGI values, it did not have the highest amount of precipitation. 2020 had fewest days of continuous snow cover (200 days), and the second-lowest quantity of rain (74.7 cm). However, a decent proportion of rain fell during the growing season (37.8%), which was March-September, when NDGI remained above 0.05 based on the remote sensing analysis of 2018-2021. 2019 had the most days of continuous snow cover (242 days), the highest amount of rain (141.8 cm), with a considerable

portion occurring during the growing season (28.1%). 2021 received the smallest amount of rainfall overall (49.6 cm), as well the lowest rainfall during the growing season (10.5 cm).

Table 5. Precipitation amount and timing in Plumas County

Year	Days of continuous snow cover	Dates of continuous snow presence	Winter (Oct-Feb) rain (cm)	Growing season (Mar-Sept) rain (cm)	Total rain (cm)
2018	219	11/4 - 6/12	49.9	48.2	98.1
2019	242	11/22 - 7/21	102.1	39.7	141.8
2020	200	11/26 - 6/12	46.5	28.2	74.7
2021	211	11/7 - 6/5	39.1	10.5	49.6
2022	209*	10/18-5/14	76.2	16.6*	92.8*

*As of May 14, 2022

The Palmer drought severity index (PDSI) data for 2018-2021 (Figure 15b) show that Plumas County experienced the most severe drought conditions in 2021, reaching values below -5 (extreme drought) in Summer 2021. A PDSI between -1.9 and +1.9 can be classified as “near normal” (NCAR. Though NDGI values were lower in 2018 and 2019, PDSI values remained in the “near normal” range during the entire growing season, winter 2019 did see values of down to -2.22 (moderate drought). The 2020 PDSI also remained in the “normal” range, though became negative throughout the year. PDSI values reached “moderate drought” levels on October 26, 2020, reaching “severe” on October 10, 2020, and “extreme” on June 29, 2021.

Figure 15. Snow and drought in Plumas County, CA (2018-2021)

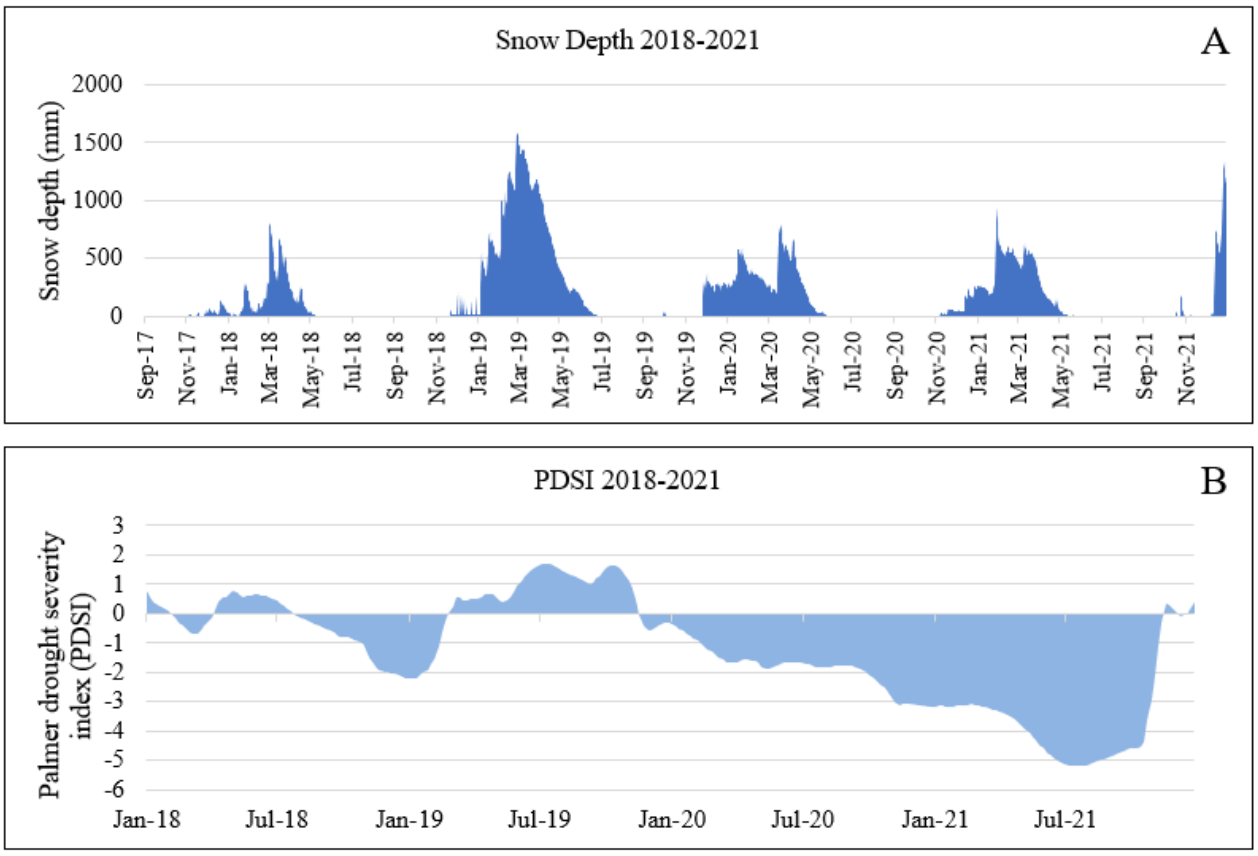

Figure 15. Climate data for Plumas County were obtained from Climate Engine (http://climateengine.org), provided by Desert Research Institute and University of Idaho. Data used included a) Snow depth (mm) (SNOWDAS) and b) PDSI (gridMET).

4. Discussion

4.1 Implications of multiscale analysis

Study of the years 2018-2021 suggest that years of severe drought are both shorter and less productive, particularly past a certain threshold of dryness. This is exemplified by the 2021 growing season, which experienced a perfect storm of dry conditions, including earlier snowmelt, low overall rain, and very little rain during the growing season, which translated to the lowest average NDGI values thorough the growing season. It remains difficult to isolate which climate variables might be most important from this limited period of study, but some relationships were observed in the 2021 growing season. In terms of climate variables, VPD emerged as a key control of plant function in a severe drought year. The strong inverse relationship between VPD and stomatal conductance ($R^2 = 0.63$) shows that high VPD limited plant growth, even with higher water availability, and was also highly significant for plant water content. This finding is supported by a previous study in a sub-Mediterranean grassland, which found that evapotranspiration responded more strongly to VPD increasing than decreasing soil water content (Noumonvi et al., 2019).

Several factors important to explaining the variation in AGB and leaf area of dominant sedges and grasses were found, including date, shallow soil moisture, plant functional group, and the interactions between these factors. Though changes in community composition were recorded in the 2021 growing season, factors most important to the herbs and rushes remain elusive, given that date and shallow soil moisture were shown to be not significant to explaining the variation in the dry weight of these plant groups.

Relationships between soil moisture (0-10 cm) and productivity were somewhat contradictory, though several results point to the potential importance of shallow soil moisture for meadow vegetation, and by extension the creek diversion, which channels soil water to this area of the meadow. The interaction between shallow soil moisture and PFG was highly significant for sedge/grass dry weight and leaf area. Further, the decreasing correlation between PWC and soil moisture at various depths indicates that most of plant available water in this period was concentrated between 0-20 cm (Table 2). Low root allocation at time of BGB sampling, possibly the result of suboptimal sampling conditions, make it hard to confidently discern relationships between biomass allocation and climate variables. However, the EFT soil moisture data shows water at 0-20 cm depths disappearing by DOY 180 and 200, which points to the use of deeper soil water. Predawn water potential, though not sampled on all dates, was also weakly correlated to plot-level shallow soil moisture. However, it is still possible that shallow soil moisture is important to overall plant productivity at RCV, though its importance may vary spatially and between species. This aligns with results of another study in the same meadow and year, which found that the availability of shallow soil moisture was most important for productivity during the growing season (Mousavi, 2022, p. 69).

NDGI analysis revealed 2020 as the most productive year in the study area from 2018-2021, despite 2019 having a longer period of snow cover, greater annual precipitation and during the growing season, all of which would be expected to bring about increased productivity. This differs from the entire meadow extent (Figure 12), for which 2019 had the highest NDGI values, indicating that 2019 had the highest productivity during the growing season at the meadow-scale. This difference could stem from a difference in plant community in the study area compared to

the entire meadow extent. Another study of species' composition at RCV for the same period (2018-2021) which sampled a nearby area of the meadow, found that patterns in plant cover differed between plant groups. Categorization was based upon the wetland indicator status groups which include the following categories: 1. Obligate, 2. Facultative wetland, 3. Facultative, 4. Facultative Upland, and 5. Upland (Lichvar et al., 2012). Of these, Obligate and Facultative Wet had the highest percent cover in 2019, followed by a decrease in 2020. In contrast, Facultative and Facultative Upland species saw a large increase in 2020 over 2019, while Upland species showed only a very slight increase (Rust, 2021). Since the NDGI values show that 2020 was more productive than 2019 in the study area, this suggests that the Facultative and Facultative Upland species that may contribute to higher productivity in the study area. This also raises questions as to the reason for this difference. One reason could be that these plant types are more heavily impacted by the legacy effect of long-term drought. 2018 and 2019 both came at the end of a historic drought lasting nearly eight years (National Integrated Drought Information System), and this may have led to a delay in the reestablishment of these plant species. In a study in an alpine grassland, a drought legacy effect of 10 months was measured (Mackie et al., 2019). In addition, a decline in certain plant communities during prolonged drought may have led to a delay in the impacts of increased water availability. For instance, higher water availability in 2019 could result in higher seed production and successful seed set in 2019, and thus more plants and higher productivity in 2020.

4.2 Assessing study design

Overall, the productivity in the sampling area represented that of the broader meadow study area, as the study area and plot NDGI were very well-correlated ($R^2 = 0.899$). In addition,

the plot and study area NDGI were well-correlated to the NDGI of the whole meadow extent (R^2 = 0.76 and 0.84, respectively). Including another portion of the of meadow with different characteristics (i.e., vegetation community, soil moisture, soil type) is likely to increase the strength of this relationship, ensuring that sampling represents the meadow at large versus its wetter parts.

The chosen VI (NDGI) performed well based on decent correlations to the several productivity variables collected in the field, including fresh plant weight (R^2 = 0.40), LAI (R^2 = 0.59), and PWC (R^2 = 0.77). The relationship was generally strongest at the growing season peak, with higher levels of water availability and vegetation greenness, decreasing as vegetation senesced. The relationship with fresh plant weight differed slightly in that there was a modest increase in R^2 between 6/2 (0.33) and 6/28 (0.40). Even at the peak of the season, standing dead matter already constituted 31.7% of cover. It seems possible that earlier in the season, or in less dry years, there might be a lower proportion of standing dead, and thus a better relationship between NDGI and plants on the ground. In addition, field data did not span the whole growing season, but captured the peak and senescence of one portion of the meadow. However, in conjunction with NDGI data, the results of this study are comparable to another study that examined productivity and phenology in RCV in 2021. Using digital repeat photography to track photosynthetic potential over time, this study established the 2021 peak as DOY 157 and the end of senescence at DOY 240 (Mousavi, 2022, p. 44-47), patterns reflected in the NDGI values (Figure 11-13).

4.3 Study limitations

There are several limitations and sources of error of this study that should be mentioned, to contextualize findings and provide an opportunity to improve future sampling efforts. Extreme heat in the field led to some underestimation of leaf area, particularly in herbs. Belowground biomass was also likely underestimated, being samples at the end of the growing season when roots are more desiccated, and the soil drier and more difficult to collect. In comparison, BGB sampling in an initial trip in May 2022 was easier to collect and appearing to capture more fine roots and soil. The grasshopper herbivory observed on 6/28 was another source of error, as its impact was not quantified and incorporated in the analysis and may lead to an underestimation of AGB accumulation.

In terms of remotely sensed data, the mismatch between dates between years means that estimates for snow duration and season timing are merely estimates. For instance, images that represented the season "peak" fell on June 14, June 19, June 8, and June 3, respectively. However, this was based on the availability of suitable imagery and the approximately monthly temporal resolution. Lastly, as NDGI values were lowest in 2021, it is possible that in more average years, AGB surpasses threshold for "dense" vegetation, which could make another VI more suitable, to ameliorate the impact of saturation.

5. Conclusion

Data collected establishes a crucial baseline of phenology, soil moisture, productivity, and community composition in the study system. In addition to laying the groundwork for future data collection in RCV, data collected contribute to the understanding of vegetation in the meadow, including its community composition, AGB values, and soil moisture in a very dry year, useful in advancing our understanding of this system and possibly similar montane meadows in the Sierra Nevada mountains. In addition, it provides clues of what more future growing seasons might look like as conditions become warmer and drier. The 2021 water year was second driest in California history, with 60% of average snowpack (CDWR 2021). Field monitoring in 2021 showed how plant community composition changed throughout the growing season, in addition to the proportion which remained photosynthetic. Several drivers emerged as controls of productivity, including shallow soil moisture and VPD. Shallow soil moisture was highly significant for the productivity of sedge/grass, the dominant plant group in RCV, and high VPD limited productivity, even with higher water availability.

Though productivity in the years studied did not correspond neatly with county-level precipitation in the relatively hydric study area, in a very dry year the peak and overall NDGI values were lower, and the growing season earlier and shorter. In comparison, NDGI values from the entire meadow relate more predictably with precipitation data, with the lowest values in the driest year (2021), and the highest in the wettest year (2019). Data from an extreme drought year allows for an improved understanding of the response of Sierran montane meadows to ongoing climate change and the degree to which restoration contributes to their resiliency.

The study design used captured meadow vegetation well and could be useful for continuing monitoring efforts. Though NDGI is a new VI not yet widely used, it served to illustrate the patterns of green-up, senescence, and greenness at RCV, exhibiting a strong overall correlation to plant water content. Future studies could explore the use of other VIs, with more frequent images and finer resolution drone data to improve correlations between field-level metrics and remotely sensed data. Vegetation dynamics in montane meadows are complex, and further study is required to make patterns clearer, and to elucidate mechanisms sufficiently to enable predictions for the future.

References

Arnold, C. L. (2014*). Coupled Hydrological and Biogeochemical Dynamics in High Elevation Meadows: Thresholds, Resiliency and Change* [Doctoral dissertation, University of California Merced]. ProQuest Dissertations and Theses.

Bussotti, F., Ferrini, F., Pollastrini, M., & Fini, A. (2014). The challenge of Mediterranean sclerophyllous vegetation under climate change: From acclimation to adaptation. *Environmental and Experimental Botany*, 103, 80-98.

California Air Resources Board. (2015). *Greenhouse Gas Reduction Fund: California Department of Fish and Wildlife Expenditure Record for Fiscal Year 2014-15 – Mountain Meadows*. Retrieved from https://ww3.arb.ca.gov/cc/capandtrade/auctionproceeds/14-15_dfw_mm_expenditure_record.pdf

CA Natural Resources Agency (2016). *California Water Action Plan 2016 Update*. California Water Library. Retrieved from https://cawaterlibrary.net/document/california-water-action-plan-2016-update/.

Cao, Feng, Y., Liu, X., Shen, M., & Zhou, J. (2020). Uncertainty of vegetation green-up date estimated from vegetation indices due to snowmelt at northern middle and high latitudes. *Remote Sensing*, 12(1), 1-20.

Chapin, F.S, Matson, P. A., & Mooney, H. A. (2002). *Principles of Terrestrial Ecosystem Ecology* (p.97-119). New York, Springer.

Cleland, E., Chuine, I., Menzel, A., Mooney, H., & Schwartz, M. (2007). Shifting plant phenology in response to global change. *Trends in Ecology & Evolution*, 22(7), 357-365.

de Castro, A.I., Shi, Y., Maja, J. M., & Peña, J. M. (2021). UAVs for Vegetation Monitoring: Overview and Recent Scientific Contributions. *Remote Sensing*, 13(11), 1-13.

National Integrated Drought Information System. *Drought in California from 2000–Present.* Retrieved from https://www.drought.gov/states/california.

Emmons, J.D. (2013). *Quantifying the restorable water volume of Sierran meadows*. [Master's dissertation, University of California Davis]. ProQuest Dissertations Publishing.

European Space Agency (ESA) (2021). *Sen2Cor Configuration and User Manual.* Retrieved from https://step.esa.int/main/snap-supported-plugins/sen2cor/sen2cor-v2-10/.

FR-CRM. (1996). *Red Clover Creek Demonstration project: Fact Sheet # 3*. Feather River Coordinated Resource Management - Plumas Corporation. Retrieved from: https://www.plumascorporation.org/uploads/4/0/5/5/40554561/redclover1985factsheet3.pdf.

FR-CRM. (2008). *Red Clover/McReynolds Creek Restoration Project - Final Report*. Retrieved from: http://www.plumascorporation.org/uploads/4/0/5/5/40554561/redcloverfinalreport01_08.pdf.

Harris, R.W. (1992). ROOT-SHOOT RATIOS. *Journal of Arboriculture* 18(1), 39-42. Retrieved from https://auf.isa-arbor.com/request.asp?JournalID=1&ArticleID=2479&Type=2.

Huntington, J., Hegewisch, K., Daudert, B., Morton, C., Abatzoglou, J., McEvoy, D., and T., Erickson. (2017). Climate Engine: Cloud Computing of Climate and Remote Sensing Data for Advanced Natural Resource Monitoring and Process Understanding. *Bulletin of the American Meteorological Society*, http://journals.ametsoc.org/doi/abs/10.1175/BAMS-D-15-00324.1

IPCC (2013) Climate change, 2013. *Near-term Climate Change: Projections and Predictability. The Physical Science Basis: Contribution of Working Group I to the Fifth Assessment Report of the Intergovernmental Panel on Climate Change*. Cambridge University Press, Cambridge, United Kingdom and New York, NY, USA.

Jonas, T., Rixen, C., Sturm, M., & Stoeckli, V. (2008). How alpine plant growth is linked to snow cover and climate variability. Journal of Geophysical Research*: Biogeosciences*, 113(G3).

Kottek, M., Grieser, J., Beck, C., Rudolf, B. and Rubel, F. (2006). World Map of the Köppen-Geiger climate classification updated. *Meteorol*. Z., 15, 259-263.

Li, P., Sayer, E.J., Jia, Z., Liu, W., Wu, Yuntao, Y., Sen, . . . Liu, L. (2020). Deepened winter snow cover enhances net ecosystem exchange and stabilizes plant community composition and productivity in a temperate grassland. *Global Change Biology*, 26(5), 3015-3027.

Lucas, R. G. (2016). *Evapotranspiration and Groundwater Patterns in Montane Meadows of the Sierra Nevada, CA* [Doctoral dissertation, University of California Merced]. ProQuest Dissertations and Theses.

Mackie, K.A., Zeiter, M., Bloor, J. M. G., Stampfli, A., & Vries, F. (2019). Plant functional groups mediate drought resistance and recovery in a multisite grassland experiment. *The Journal of Ecology*, 107(2), 937–949.

Martin, C., Simonin, K.A., Oliphant, A.J., & Baguskas, S.A. (2021, December 1). *Impacts of Drought and Restoration on Montane Meadow Plant Phenology and Productivity* [Poster]. AGU Fall meeting, 2021. Accessed from https://sfsu.box.com/s/om04eccstu7s84633ezdv2tbshify1du

Mousavi, S. (2022). *Assessing Meadow Carbon Cycling Using Digital Repeat Photography and Eddy Covariance Techniques* [Master's dissertation, San Francisco State University]. Retrieved from https://geog.sfsu.edu/thesis/using-digital-repeat-photography-and-eddy-covariance-techniques-assess-red-clover-valley.

National Center for Atmospheric Research (NCAR). *Climate Data: PALMER DROUGHT SEVERITY INDEX (PDSI).* Retrieved from https://climatedataguide.ucar.edu/climate-data/palmer-drought-severity-index-pdsi

National Weather Service (NWS). NowData records for Portola, CA. Accessed November 23, 2021.

Noumonvi, K., Ferlan, M., Eler, K., Alberti, G., Peressotti, A., & Cerasoli, S. (2019). Estimation of Carbon Fluxes from Eddy Covariance Data and Satellite-Derived Vegetation Indices in a Karst Grassland (Podgorski Kras, Slovenia). *Remote Sensing* (Basel, Switzerland), 11(6), 649–.

Rust, T. (2021). *Clover Valley Ranch: 2021 Vegetation Monitoring.* The Sierra Fund.

Sloat, L., Henderson, L., Lamanna, A., & Enquist, N. (2015). The Effect of the Foresummer Drought on Carbon Exchange in Subalpine Meadows. *Ecosystems*, 18(3), 533-545.

Tempfli, K., Kerle, N., Huunerman, G.C., & Janssen, L.L.F (eds.) (2009). *Principles of Remote Sensing* (4th ed., p. 149). Enschede, The Netherlands: ITC.

The Sierra Fund (2018). *CDFW GGRF Full Proposal, Form 2: Site description and maps.*

USGS. *Landsat Surface Reflectance-derived Spectral Indices*. Retrieved from https://www.usgs.gov/core-science-systems/nli/landsat/landsat-surface-reflectance-derived-spectral-indices?qt-science_support_page_related_con=0#qt-science_support_page_related_con.

Robert W. Lichvar, R.W., Melvin, N.C., Butterwick, M. L., & Kirchner, W.N. (2012). *National Wetland Plant List Indicator Rating Definitions*. U.S. Army Corps of Engineers.

Retrieved from https://www.fws.gov/wetlands/documents/National-Wetland-Plant-List-Indicator-Rating-Definitions.pdf.

Wang, Hao, Liu, Huiying, Cao, Guangmin, Ma, Zhiyuan, Li, Yikang, Zhang, Fawei, . . . He, Jin-Sheng. (2020). Alpine grassland plants grow earlier and faster but biomass remains unchanged over 35 years of climate change. *Ecology Letters*, 23(4), 701-710.

Wild Fish Habitat Initiative (2007). *Red Clover Creek Demonstration Project*. Montana Water Center. Retrieved from: https://archive.ph/20121211094614/http://wildfish.montana.edu/Cases/browse_details.asp?ProjectID=44.

Xu, Wang, C., Chen, J., Shen, M., Shen, B., Yan, R., Li, Z., Karnieli, A., Chen, J., Yan, Y., Wang, X., Chen, B., Yin, D., & Xin, X. (2021). The superiority of the normalized difference phenology index (NDPI) for estimating grassland aboveground fresh biomass. *Remote Sensing of Environment*, 1-14.

Yang, W., Kobayashi, H., Wang, C., Shen, M., Chen, J., Matsushita, B., Tang, Y., Kim, Y., Bret-Harte, M. S., Zona, D., Oechel, W., & Kondoh, A. (2019). A semi-analytical snow-free vegetation index for improving estimation of plant phenology in tundra and grassland ecosystems. *Remote Sensing of Environment*, 228, 31–44.

Zhou, Y., Zhang, L., Xiao, J., Chen, S., Kato, T., & Zhou, G. (2014). A Comparison of Satellite-Derived Vegetation Indices for Approximating Gross Primary Productivity of Grasslands. *Rangeland Ecology & Management*, 67(1), 9–18.

Appendix A: List of VIs and formulas from studies reviewed

NDVI	Normalized difference vegetation index	NDVI = NIR – red / NIR + red
NDII	Normalized difference infrared index	NDII = NIR – red / NIR + red
DVI	Difference vegetation index	DVI = NIR – red
DVI+	“	DVI+ = N, G (reflectance of red band on line) – red (actual reflectance)
NIRv	Near infrared reflectance of vegetation	NIRv = NDVI × NIR
RVI	Ratio vegetation index	RVI = NIR/red
EVI	Enhanced vegetation index	EVI = green × ((NIR - red) / (NIR + C1* × red – C2* × blue + L*))
EVI2	Enhanced vegetation index 2	EVI2 = 2.5(NIR – red / NIR + 2.4red + 1)
EVI3	Enhanced vegetation index 3	EVI3 = Gain factor × (NIR - red) / (NIR + C1red* – C2blue* + L*)
PI	Phenology index	PI = NDVI – NDII
PPI	Plant phenology index	PPI = – K* × ln(M* – DVI / M* – DVIsoil)
NDGI	Normalized difference greenness index (MODIS)	NDGI = 0.65 × green + 0.35 x NIR – red / 0.65 × green + 0.35 × NIR + red
NDPI	Normalized difference phenology index	NDPI = NIR – (0.74 × red + 0.26 × SWIR) / NIR + (0.74 × red + 0.26 × SWIR)
NDSVI	Normalized difference senescent vegetation index	NDSVI = SWIR – red / SWIR + red
MNDWI	Modified normalized difference water index	MNDWI = (Green - SWIR) / (Green + SWIR)
LSWI	Land surface water index	LSWI = NIR – SWIR / NIR + SWIR
RVI	Ratio vegetation index	RVI = NIR / red
ARVI	Atmospherically resistant vegetation index	ARVI = (NIR + 2 red + blue) / (NIR + 2 red – blue)
SAVI	Soil-adjusted vegetation index	SAVI = ((NIR - red) / (NIR + red + L*)) × (1 + L*)
SAVI2	“	SAVI = ((NIR - red) / (NIR + red + L*)) × (1 + L*)
MSAVI	Modified soil adjusted vegetation index	½ × [2 × NIR + 1) – (√(2 × NIR + 1)² – 8 × (NIR – red))]
OSAVI	Optimized soil adjusted vegetation index	NIR – red / NIR + red + X (X = 0.16)
RSR	Reduced simple ratio	RSR = NIR / red × [1 – (SWIR - SWIRmin) / (SWIRmax - SWIRmax)] (Uses MODIS SWIR band 5)

RSR2	Reduced simple ratio 2	Same as above. Uses MODIS SWIR band 6.
RSR3	Reduced simple ratio 3	Same as above. Uses MODIS SWIR band 7.

L = soil brightness correction factor (USGS)

C = coefficients for atmospheric resistance (USGS)

C1, C2= coefficients of aerosol resistance term (Zhou et al, 2014)

M= max DVI calculated from canopy reflectance model simulation (Yang et al., 2019)

K = gain factor, calculated from M and solar zenith angle (Yang et al., 2019)

Appendix B: Remote sensing image processing workflow

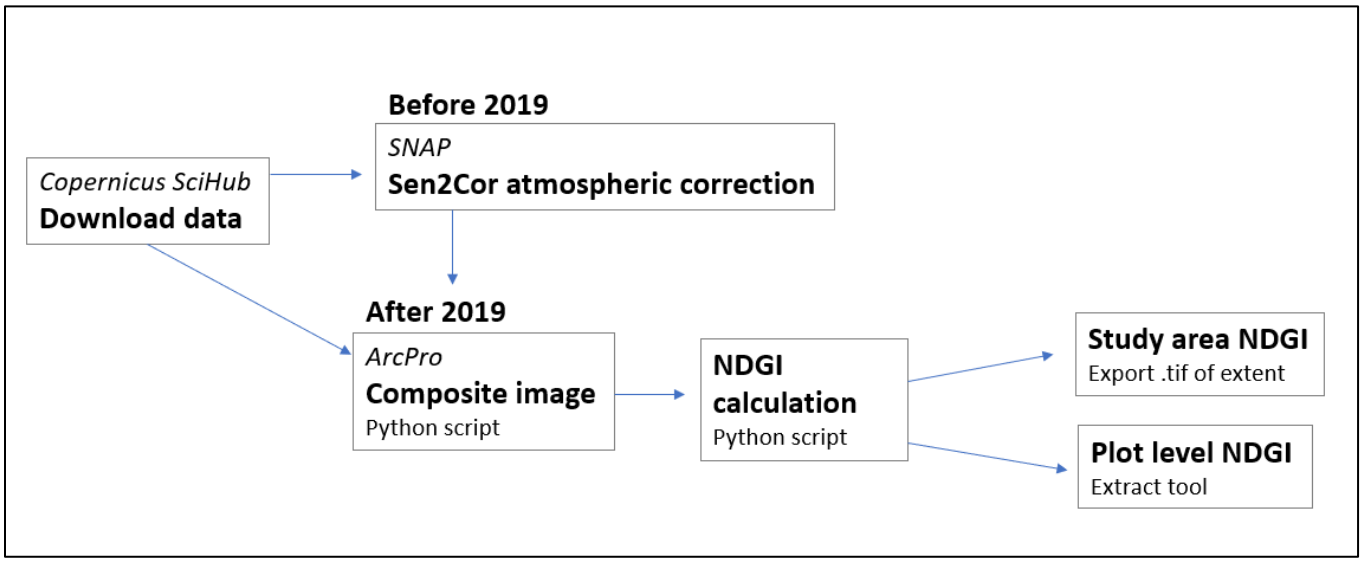

Appendix C: Supporting formulas and figures

Page 19

Formula: model=lm(dry_wt_g ~ PFG + doy + PFG*doy)

Model R^2	**Model p-value**
0.42	$1.33e^{-12}$
Coefficients	**p-value**
PFGSG	0.0002
PFGSG:doy	0.006

Page 21

Formula: model=lm(dry_wt_g~sm_vwc*PFG)

Model R^2	**Model p-value**
0.44	$3.37e^{-13}$
Coefficients	**p-value**
PFGSG	0.0313
sm_vwc:PFGSG	0.0010

Page 22

Formula: model=lm(LA~PFG*doy)

Model R^2	**Model p-value**
0.51	$2.725e^{-16}$
Coefficients	**p-value**
PFGSG	$2.40e^{-07}$
PFGSG:doy	$1.22e^{-05}$

Formula: model=lm(LA~PFG*doy)

Model R^2	**Model p-value**
0.48	$6.821e^{-15}$
Coefficients	**p-value**
sm_vwc:PFGSG	$2.725e^{-16}$

Page 24

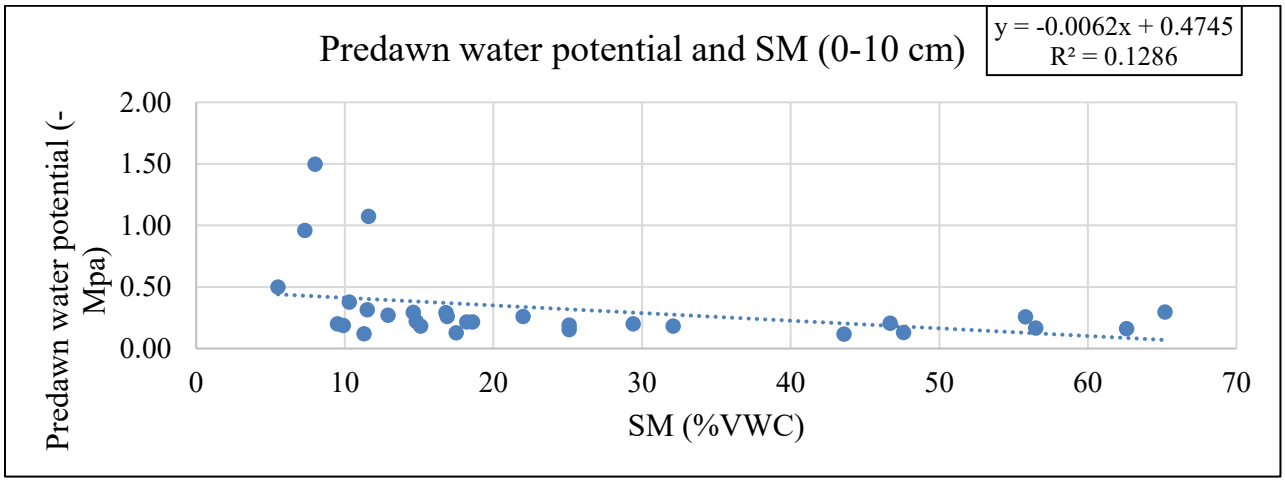
Predawn water potential and SM (0-10 cm)
y = -0.0062x + 0.4745
R² = 0.1286
Predawn water potential (-Mpa)
2.00
1.50
1.00
0.50
0.00
0
10
20
30
40
50
60
70
SM (%VWC)

Page 29

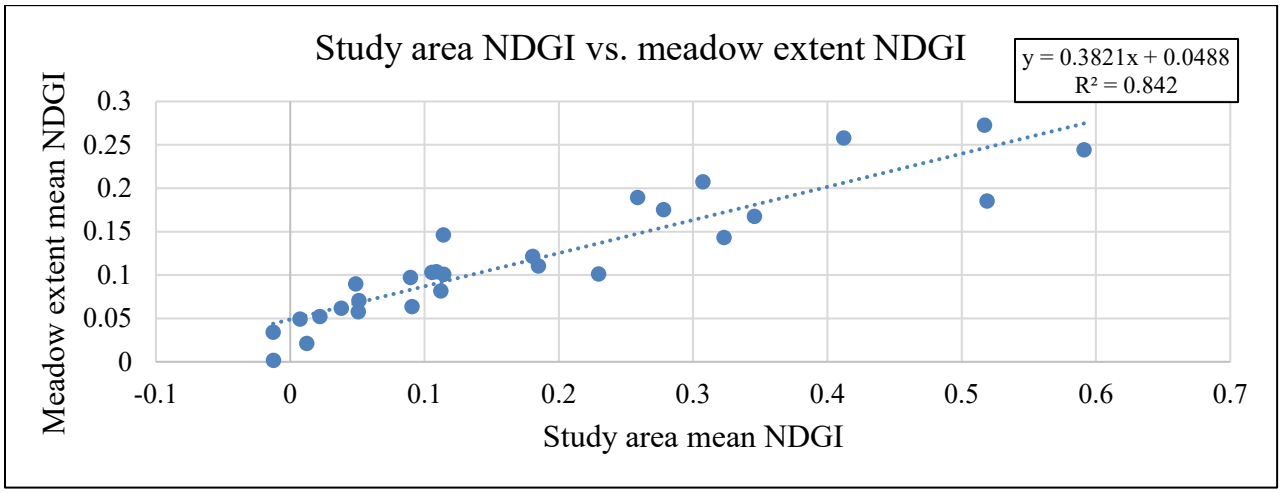
Study area NDGI vs. meadow extent NDGI
y = 0.3821x + 0.0488
R² = 0.842
Meadow extent mean NDGI
0.3
0.25
0.2
0.15
0.1
0.05
0
-0.1
0
0.1
0.2
0.3
0.4
0.5
0.6
0.7
Study area mean NDGI

Page 32

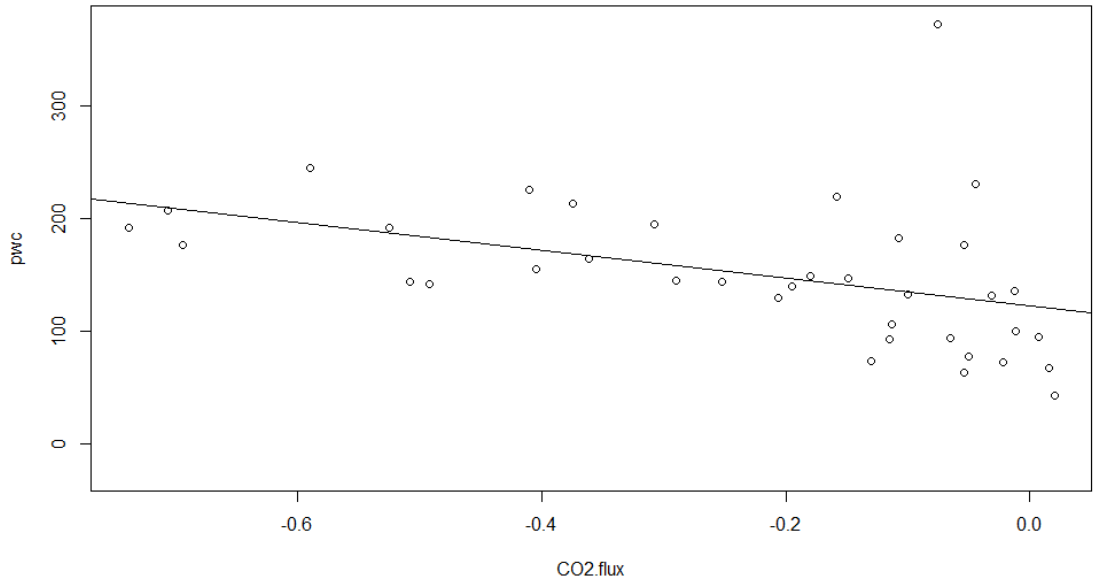

Formula	lm=lm(pwc~CO2.flux)
R^2	0.16
p-value	0.008

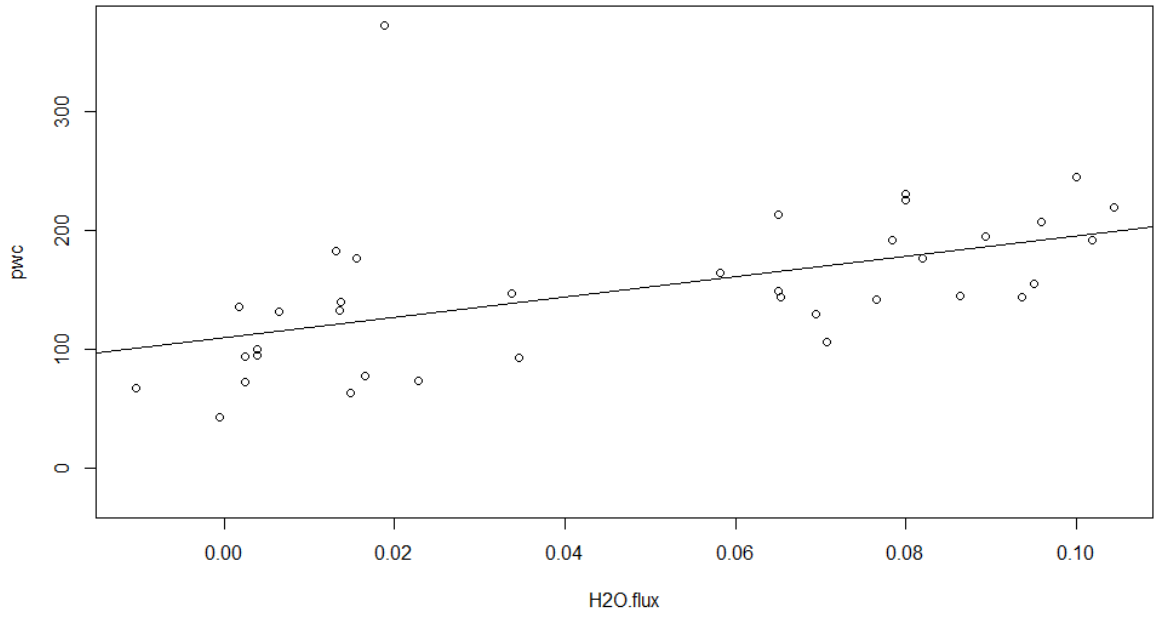

Formula	lm=lm(pwc~H2O.flux)
R^2	0.24
p-value	0.001

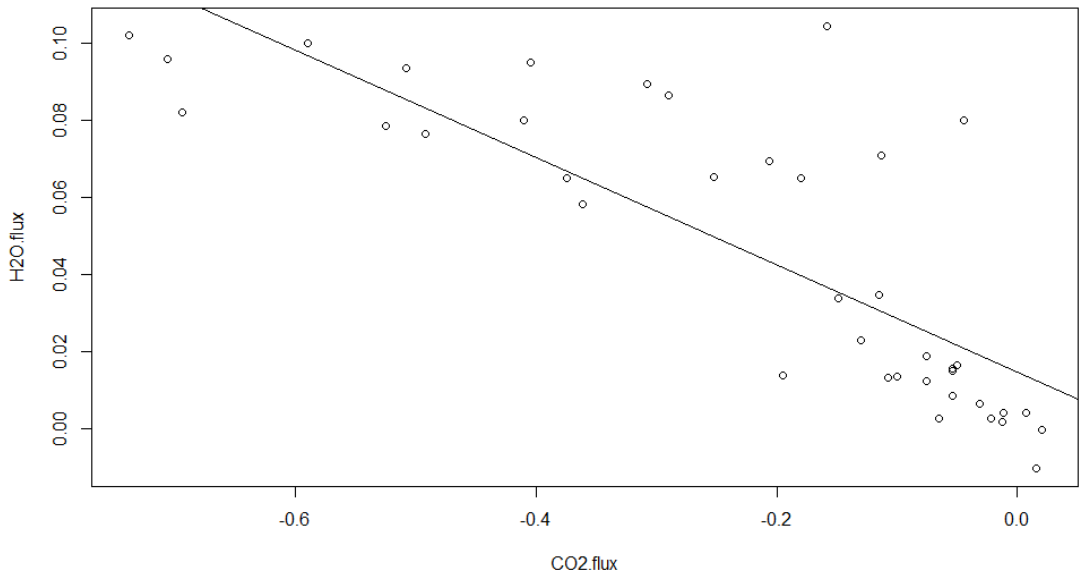

Formula	H2O.flux~CO2.flux
R^2	0.64
p-value	$2.939e^{-10}$